Astronomy & Astrophysics manuscript no. 25882a
August 17, 2015

2dF-AAOmega spectroscopy of massive stars in the Magellanic Clouds

The north-eastern region of the Large Magellanic Cloud⋆

C. J. Evans[1], J. Th. van Loon[2], R. Hainich[3] & M. Bailey[4, 2]

[1] UK Astronomy Technology Centre, Royal Observatory, Blackford Hill, Edinburgh, EH9 3HJ, UK
[2] Astrophysics Group, School of Physical & Geographical Sciences, Lennard-Jones Laboratories, Keele University, ST5 5BG, UK
[3] Institute for Physics and Astronomy, University of Potsdam, 14476 Potsdam, Germany
[4] Astrophysics Research Institute, Liverpool John Moores University, Liverpool Science Park ic2, 146 Brownlow Hill, Liverpool L3 5RF, UK

ABSTRACT

We present spectral classifications from optical spectroscopy of 263 massive stars in the north-eastern region of the Large Magellanic Cloud. The observed two-degree field includes the massive 30 Doradus star-forming region, the environs of SN1987A, and a number of star-forming complexes to the south of 30 Dor. These are the first classifications for the majority (203) of the stars and include eleven double-lined spectroscopic binaries. The sample also includes the first examples of early OC-type spectra (AAΩ 30 Dor 248 and 280), distinguished by the weakness of their nitrogen spectra and by C IV λ4658 emission. We propose that these stars have relatively unprocessed CNO abundances compared to morphologically normal O-type stars, indicative of an earlier evolutionary phase. From analysis of observations obtained on two consecutive nights, we present radial-velocity estimates for 233 stars, finding one apparent single-lined binary and nine ($>3\sigma$) outliers compared to the systemic velocity; the latter objects could be runaway stars or large-amplitude binary systems and further spectroscopy is required to investigate their nature.

Key words. galaxies: Magellanic Clouds – stars: early-type – stars: fundamental parameters – open clusters and associations: individual: NGC 2060, NGC 2070, LHA 115-N 154, LHA 115-N 158, LHA 115-N 160

1. Introduction

Our knowledge of the massive-star populations of the Magellanic Clouds has increased significantly over the past decade, largely via observations with multi-object spectrographs (e.g. Massey & Olsen 2003; Evans et al. 2004, 2006, 2011; Fariña et al. 2009; Lamb et al. 2013). Such surveys have been used to address questions pertaining to stellar evolution (e.g. Massey & Olsen 2003; Evans et al. 2008), wide-area studies of stellar kinematics (e.g. Evans & Howarth 2008), the formation of massive stars in relative isolation (e.g. Lamb et al. 2010; Bressert et al. 2012; Oey et al. 2013), the structure of stellar clusters (e.g. Hénault-Brunet et al. 2012a,b), the properties of the interstellar medium in the Clouds (e.g. Welty et al. 2006; van Loon et al. 2013), and, via multi-epoch observations, the binary properties of massive stars (e.g. Bosch et al. 2009; Sana et al. 2013; Dunstall et al. 2015).

The compendia of known spectral types of massive stars in the Clouds by Bonanos et al. (2009, 2010) emphasised the disparity in our knowledge of the spectral content of the Clouds, with classifications for 5324 stars in the Small Magellanic Cloud (SMC), but only 1750 in the Large Magellanic Cloud (LMC). Filtering the LMC catalogue from the Magellanic Clouds Photometric Survey (MCPS, Zaritsky et al. 2004) by a faint magnitude limit of $V = 15.3$ mag and a colour cut of $(V - I) < 0.0$ mag to identify likely O- and luminous B-type objects gives a total of $\sim$10 000 stars[1]. The true number of early-type stars in the LMC will be influenced by the effects of crowding in the MCPS photometry and the number of interlopers included via the above filters, but there clearly remains much to learn about the massive-star content of the LMC, even in light of recent classifications for 780 O- and B-type stars in 30 Doradus (Walborn et al. 2014; Evans et al. 2015).

In this article we present spectroscopy from observations in early 2006 (P.I. van Loon) to test the capabilities of the then new AAOmega spectrograph (Saunders et al. 2004; Sharp et al. 2006) on the 3.9 m Anglo-Australian Telescope (AAT). Two fields were observed in the LMC, one in the NE near the massive 30 Doradus star-forming region and a second in the NW, centred on the N11 region. Spectra for thirteen of the targets have been published to date: seven peculiar 'nfp' stars (Walborn et al. 2010), a massive runaway O2-type star (Evans et al. 2010), and five eclipsing binary systems (Muraveva et al. 2014). Partly motivated by results from the VLT-FLAMES Tarantula Survey

Send offprint requests to: chris.evans@stfc.ac.uk

⋆ Copies of the spectra are available at the CDS via anonymous ftp to cdsarc.u-strasbg.fr (130.79.128.5) or via http://cdsweb.u-strasbg.fr/cgi-bin/qcat?J/A+A/

[1] In this illustrative calculation we adopt an absolute magnitude for a B0 dwarf of -3.6 (Walborn 1972), a modest extinction of $A_V = 0.4$ mag (from a typical reddening toward the LMC of $E(B - V) \sim 0.13$ mag from Massey et al. 1995, and assuming R, the ratio of total-to-selective extinction of 3.1), and a distance modulus to the LMC of 18.5 mag (Pietrzyński et al. 2013).

(VFTS, Evans et al. 2011) regarding runaway stars (Evans et al. 2010, 2015), we have revisited the AAOmega data in the NE field to investigate the spectral content and dynamics of massive stars in this part of the LMC.

In this paper we present spectral classifications for 263 stars in the north-eastern region of the LMC, only 60 (23%) of which have previous classifications (and often from observations of much lower quality and/or resolution). We describe the characteristics and reductions of the observations, including the optical photometry of our sources, in Section 2. The spectral classifications of our targets are discussed in Section 3, and estimates of stellar radial velocities (RVs) are presented in Section 4, followed by a short summary in Section 5. The observations in the field centred on the N11 region will be presented in a future article.

2. Observations

AAOmega is a fibre-fed, twin-arm spectrograph, with light separated into blue and red arms using a dichroic beam splitter (Saunders et al. 2004; Sharp et al. 2006). Up to 392 objects across a field on the sky that is 2° in diameter can be observed simultaneously, using fibres on the prime-focus focal plate configured with the robotic positioner of the Two-degree Field facility (2dF, Lewis et al. 2002); each fibre has an on-sky aperture of 2″. Targets are selected in the 2° field using the CONFIGURE software (see Lewis et al. 2002).

Luminous early-type stars were selected as potential targets from the MCPS (Zaritsky et al. 2004) using a magnitude cut of $V < 14$ mag (to ensure a signal-to-noise ratio of >50) and a colour cut of $(V - I) < 0.0$ mag to identify early-type stars. We used CONFIGURE to select targets from our input list using a field centre of $\alpha = 05^{\rm h}\,36^{\rm m}\,07^{\rm s}$, $\delta = -69°\,15'\,58''$ (J2000). For context, these coordinates are 3′ NE of the Honeycomb nebula (Wang 1992), 3.′5 E of SN1987A, and 17′ SW of R136 (the massive cluster at the centre of 30 Dor). The large field (2° diameter) enabled us to observe a reasonable number of targets in the regions immediately south of 30 Dor (including NGC 2060), in the N154, N158, and N160 complexes further to the south (Henize 1956), and field stars across the region. To illustrate the distribution of our targets, their locations are overlaid on the Digitized Sky Survey (blue-optical) image in Figure 1.

The NE LMC field was observed on 2006 February 22–23. The data presented here were obtained with the blue arm, using the 1700B grating on the first night, and the 1500V grating on the second. Simultaneous observations were obtained with the red arm using the 1700D grating and centred at 8620 Å; this region contains fewer lines of interest for massive stars than the blue spectra so these data were not considered further.

The data were reduced using the 2DFDR software (Lewis et al. 2002). In brief, 2DFDR was used for bias subtraction, fibre location, extractions, division by a normalised flat-field, and wavelength calibration of each target. Subsequent processing included correction of the spectra to the heliocentric frame, sky subtraction, rejection of significant cosmic rays, and preliminary normalisation (using pre-defined continuum regions). The delivered spectral coverage and resolution from the observations with the blue arm of the spectrograph is summarised in Table 1. The signal-to-noise ratio of the final spectra obtained with the 1700B grating is 50-60 per rebinned pixel for the faintest targets, and in excess of 100 for the brightest supergiants. The signal-to-noise ratio of the (longer and slightly lower resolution) 1500V observations is typically 20-30 greater than for the 1700B data.

Table 1. AAOmega spectrograph settings used.

Grating	$\lambda_{\rm c}$	λ-coverage	$\Delta\lambda$(FWHM)		Exp.
	[Å]	[Å]	[Å]	[pix.]	[s]
1700B	4100	3765–4400	1.00	3.05	2×600
1700B	4700	4375–4985	1.00	3.05	2×600
1500V	4375	3975–4755	1.25	3.25	2×900

Astrometry and optical photometry for each target (from the MCPS) is listed in Tables 2 and 3, respectively (both available online) – the identifiers in the first column are simply the running numbers (in ascending RA) from our list of potential targets (hence those observed do not run in a continuous sequence); for consistency with the identifications used by Walborn et al. (2010) we also adopt them here. We note that the majority of the photometry from Zaritsky et al. for stars with $V < 13.5$ mag was taken from the survey by Massey (2002), which employed a photometric aperture of 16.″2; thus in many instances crowding and/or nebular contamination may well influence the values in Table 3 (e.g. see discussion by Evans et al. 2011). Cross-matches of our targets with identifications/aliases from past spectroscopy are included in the final column of Table 2.

3. Spectral classification

The AAOmega spectra were classified by visual inspection in comparison with standards following the usual precepts for early-type stars (Walborn & Fitzpatrick 1990; Sota et al. 2011, 2014), taking into account the reduced metallicity of the LMC (e.g. Fitzpatrick 1988; Walborn et al. 1995, 2014; Evans et al. 2015), the effects of rotational broadening and the spectral resolution of our data. In brief, the primary diagnostic lines in the O-type spectra are the ionisation ratios of the helium lines, while also taking into account absorption from Si III at the latest types. The additional qualifiers employed in the classifications are summarised in Table 3 of Sota et al. (2011), and the spectral-type and luminosity-class criteria used for the later types are those summarised in Tables 4, 5, and 6 of the same study. The B-type classifications employed the same spectral-type criteria as those in Tables 1 and 2 of Evans et al. (2015), with luminosity classes assigned from the width of the Balmer lines, while also taking into account the intensity of the silicon absorption lines at the earlier types; example sequences for O- and B-type spectra were given by Sota et al. (2011) and Evans et al. (2015), respectively.

The classifications of the AAOmega spectra are listed in Table 2, representing the first classifications for 203 of our targets. Previous classifications for the remaining 60 stars are summarised in Table 4 (available online and complete to the best of our knowledge); in many cases the AAOmega spectra are superior to past spectroscopy, e.g. the resolution of the spectra obtained by Testor & Niemela (1998) was only 8 Å. Initial inspection of the spectra revealed eleven double-lined binaries (SB2s), and a number of candidate single-lined binaries (SB1s), discussed further in Section 6.

Our classifications of the B-type supergiants include suffixes to indicate nitrogen lines which are strong (Nstr) or weak (Nwk) compared to morphologically-normal stars of the same adopted spectral type. These qualifiers were diagnosed from visual inspection of the CNO absorption features throughout the spectra, but principally informed by the intensity of the N II λ3995 and the CNO features in the $\lambda\lambda$4640–4650 region (Walborn 1976; Fitzpatrick 1991). An example of the contrast between Nstr and

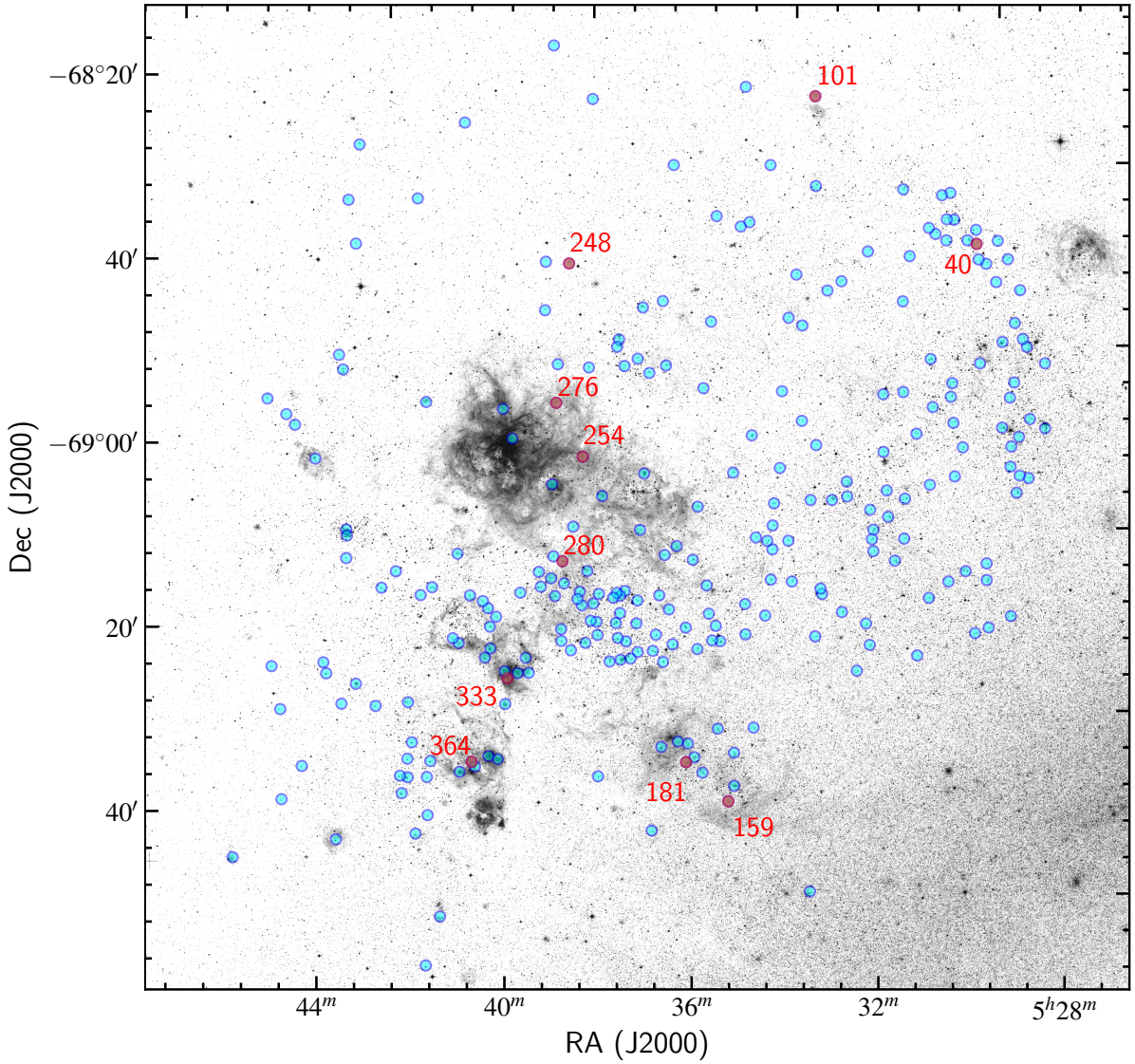

Fig. 1. Location of our AAOmega targets overlaid on a blue-optical image from the Digitized Sky Survey (DSS). The ten early-type stars (with classifications of O4 or earlier) discussed in Section 3 are highlighted in red.

Nwk spectra of B-type supergiants is given in Figure 1 of Evans et al. (2015).

The sample includes ten stars with classifications of O4 or earlier and their spectra are shown in Figure 2. Four of these were previously unknown, namely: AAΩ 30 Dor 101, 181, 248, and 280. Given the absence of He I λ4471 in the spectrum of AAΩ 30 Dor 159, we adopt a classification of O3.5 III(f*) over the O4 III(f) from Walborn et al. (2002a). The sample also includes examples of the nfp class of peculiar O-type spectra, which are defined by composite emission and absorption in the He II λ4686 line (Walborn 1973). The six nfp stars in the sample, AAΩ 30 Dor 142, 187, 320, 333, 368 and 380, were included in the discussion of the phenomenon by Walborn et al. (2010), and we adopt their classifications here.

The classification of AAΩ 30 Dor 078 (SOI 399, Stock et al. 1976) also merits brief discussion. Classified as A0 Ia by Stock et al., its classification here as B3 Iab is tantalising in the context of variations associated with luminous blue variables. The objective-prism spectroscopy used by Stock et al. was relatively coarse in terms of spectral resolution, but it is notable that their classifications include spectra as early as B6 (for comparable magnitudes and from the same photographic plate), so it is plausible to assume that they would have been able to distinguish SOI 399 as a B-type spectrum if it was in the same state as the 2006 observations[2]. Checks of the ASAS-3 database (spanning

[2] Stock et al. (1976) cross-matched their star 399 to Sk−68° 100, but Brian Skiff's updated catalogues (see footnotes to Table 2) match this Sanduleak source to SOI 398 (classified by Stock et al. as A1 Ia).

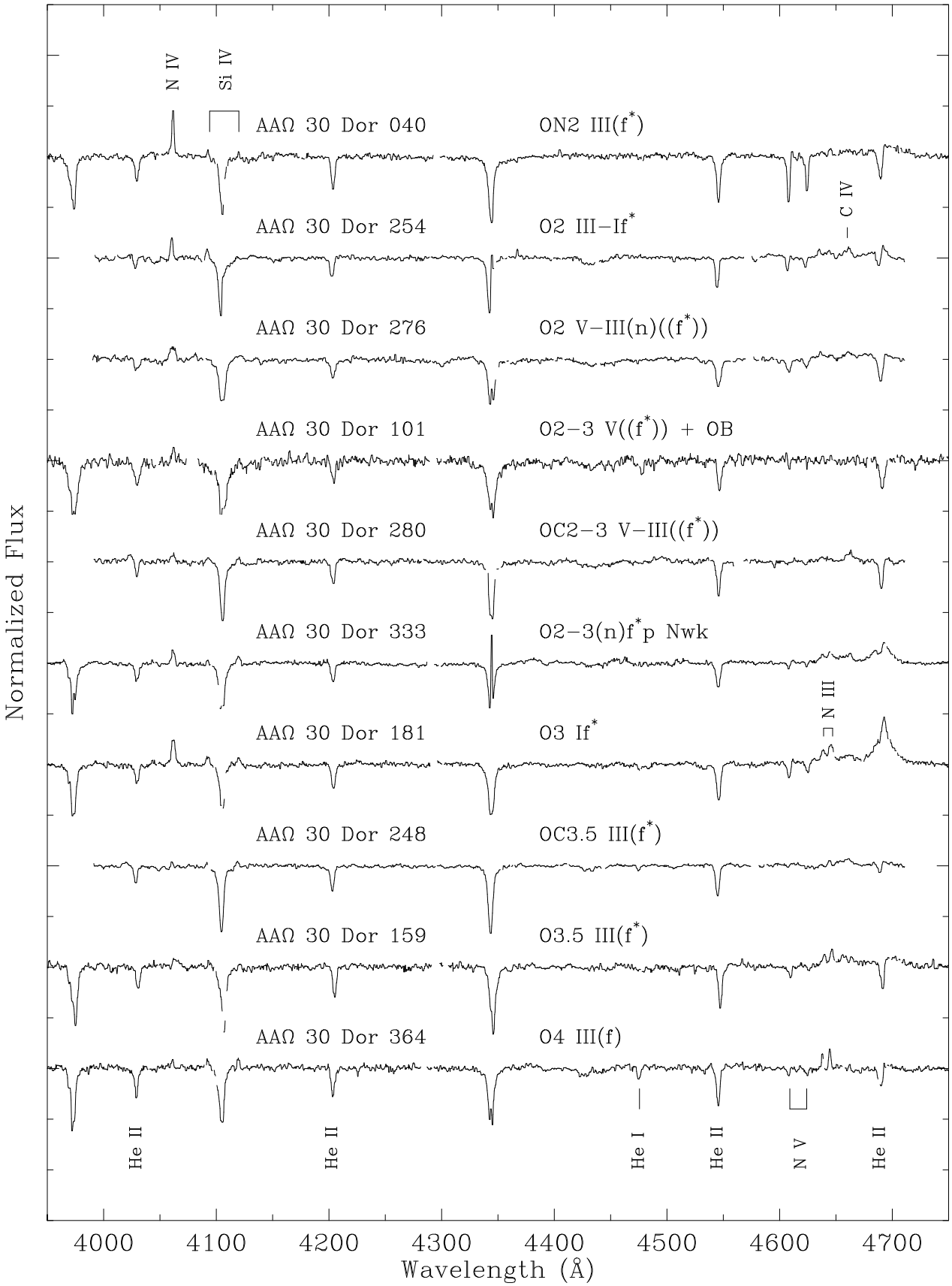

Fig. 2. AAOmega spectra of the ten early O-type stars in the sample (with each spectrum smoothed by a 5-pixel median filter for clarity and offset by 0.5 continuum units). Absorption lines identified in the spectrum of AAΩ 30 Dor 364 are: He II $\lambda\lambda$4026, 4200, 4542, 4686; He I λ4471; N V $\lambda\lambda$4604, 4620. The emission lines identified in the spectra are, in order of increasing wavelength: N IV λ4058; Si IV $\lambda\lambda$4089, 4116; N III $\lambda\lambda$4634-40-42; C IV λ4658. Broad absorption from the λ4430 diffuse interstellar band can be seen in some spectra (e.g. AAΩ 30 Dor 254).

2000–2009, see Pojmański 2002) and the DASCH archive (spanning 1890–1990, Grindlay et al. 2012) reveal no significant photometric variations (given the cadence of the available data).

3.1. Indications of CNO abundances in early O-type stars

From inspection of the spectra in Figure 2 we noted the apparent weakness of the nitrogen features in AAΩ 30 Dor 248 and 280. These lines are the primary classification criteria at such early types (see Walborn et al. 2002a), yet in these two spectra there is only weak/marginal N III $\lambda\lambda$4634-40-42 and N IV λ4058 emission, and an absence of N V $\lambda\lambda$4604-4620 absorption. The absence/weakness of He I λ4471 (and other He I features) argues for the early-types adopted here, and we suggest these are the nitrogen-poor counterparts of the morphologically normal and nitrogen-rich O2-type stars discussed by Walborn et al. (2004).

Nitrogen enrichment/deficiency in the spectra of late O- and early B-type spectra was first noted by Walborn (1976), primarily with reference to the absorption strengths of the CNO features in the $\lambda\lambda$4640–4650 region. At earlier types, from both morphlogical considerations and quantitative analysis, Walborn et al. (2004) argued that some O2-type spectra (classified as ON2) are nitrogen-rich compared to morphologically normal O2-type spectra, suggesting a more advanced evolutionary state or greater chemical enrichment via initially-larger rotational velocities.

By analogy to the ON/OC sequence at later types (e.g. Walborn 1976; Sota et al. 2011), we therefore classify AAΩ 30 Dor 248 and 280 as OC-type spectra. As well as the chemical abundances, a broad range of physical factors (e.g. gravity and mass-loss rate) influence the appearance of the nitrogen features in the earliest O-type stars (Rivero González et al. 2012). On morphological grounds we employ the OC classification for the two spectra with an absence of N V $\lambda\lambda$4604, 4620 absorption, combined with C IV λ4658 emission. In addition, the weak but still discernable N V absorption in the spectrum of AAΩ 30 Dor 333 argues for an Nwk qualifier (Walborn, priv. comm.). As at later types, we suggest that AAΩ 30 Dor 248 and 280 could be examples of an earlier evolutionary stage (i.e. less chemical processing/enrichment) than the morphologically-normal objects such as AAΩ 30 Dor 254, with the ON2 star, AAΩ 30 Dor 040, completing the sequence. To highlight the trend in the N V absorption lines in this sequence (and the presence of C IV emission), a subset region of the AAOmega spectra for three stars is shown in Fig. 3.

Pending further observations (including the Hα profiles to constrain the wind properties), we calculated investigative synthetic spectra using the PoWR model atmosphere code (Hamann 2003, 2004). Initially developed for analysis of Wolf–Rayet type spectra, the code is also well suited for analysis of O-type stars (e.g. Oskinova et al. 2007; Evans et al. 2012). Adopting the physical properties from the published analysis of VFTS 016 (i.e. AAΩ 30 Dor 254) from Evans et al. (2010), we calculated seven PoWR models to investigate if the C IV λ4658 line is genuinely sensitive to abundance, or if it is significantly affected by other physical parameters.

The baseline model parameters were: an effective temperature ($T_{\rm eff}$) of 50 kK, luminosity (L) of $\log(L/L_{\odot}) = 6.08$, gravity ($g_{\rm grav}$) of $\log g_{\rm grav} = 3.75$, microturbulence (ξ) of 30 km s^{-1}, and a stellar wind with a terminal velocity (v_{∞}) of 3450 km s^{-1}, an acceleration law described by a β parameter of 1.0, and with a mass-loss rate ($\dot{M}$) of $10^{-5.5}\,M_{\odot}$ yr^{-1}. Chemical abundances (by mass fraction) were $X_{\rm H} = 0.7374$, $X_{\rm He} = 0.258$, $X_{\rm N} = 0.0008$, $X_{\rm C} = 0.0008$, $X_{\rm O} = 0.0016$. In the six panels of Figure 4 we show the effects, from top to bottom, of reducing the mass-loss rate to $10^{-7}\,M_{\odot}$ yr^{-1}, reducing the terminal velocity to 1000 km s^{-1}, introducing a clumped wind with a volume-filling factor, $f = 0.1$ (i.e. 10%), decreasing the microturblence to 15 km s^{-1}, reducing the iron abundance by a factor of two, and reducing the carbon abundance by a factor of ten; changing β by ± 0.2 also had minimal impact. All of the spectra have been convolved with a rotational broadening profile of 150 km s^{-1}, to match that adopted by Evans et al. (2010). These preliminary tests suggest that the carbon abundance is the principal factor influencing the appearance of the C IV line (for this adopted temperature and luminosity), and that our hypothesis of these stars as carbon-rich (relative to nitrogen) is plausible[3].

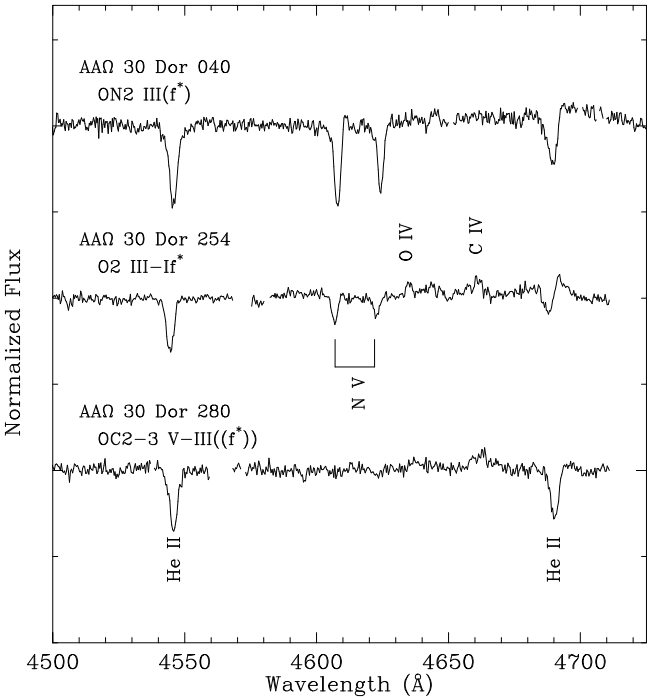

Fig. 3. $\lambda\lambda$4500-4725 range of three early-type AAOmega spectra, illustrating the large variations in N V $\lambda\lambda$4604-20 absorption and the presence of C IV λ4658 (and O IV λ4632) emission.

4. Stellar radial velocities

To estimate RVs for the O- and B-type stars we used Gaussian fits of the absorption lines listed in Table 5. The lines selected are those used by Sana et al. (2013) and Evans et al. (2015) to analyse the VFTS data, although we chose not to use He λ4026 (blend of He I and II) nor He I λ4121 (blend with O II). We note that He I λ4471 was also avoided as it is typically the line most affected by nebular contamination, and also presents other discrepancies for RV estimates, probably due to its nature as a triplet transition and a possible blend with O II (for further discussion see Appendix B of Sana et al. 2013).

[3] The PoWR models are not tailored to fit our spectra (e.g. in contrast to the observations, the N V lines are predicted in emission for the adopted parameters); our objective was a first investigation of the sensitivity of the C IV emission to different parameters.

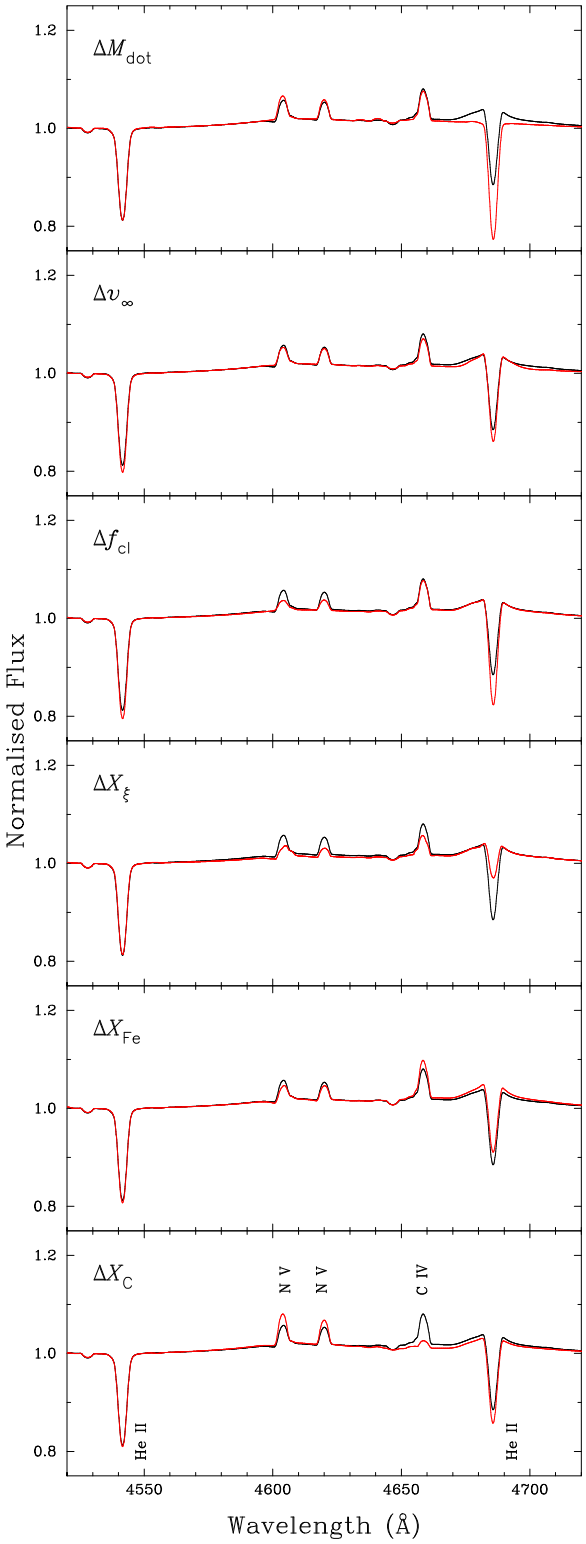

Fig. 4. Synthetic PoWR spectra (black line) adopting parameters for AAΩ 30 Dor 254 from Evans et al. (2010). The spectra plotted in red, moving from the top to bottom, are models which vary the mass-loss rate ($M_{\rm dot}$), terminal velocity (v_∞) clumping factor ($f_{\rm cl}$), microturbulence (ξ), iron abundance ($X_{\rm Fe}$, to investigate possible blanketing effects), and carbon abundance ($X_{\rm C}$), as detailed in Section 3.1. The lines identified in the lower panel are He II $\lambda\lambda$4542, 4686; N V $\lambda\lambda$4604-20, and C IV λ4658.

Table 5. Rest wavelengths used for the radial-velocity estimates. Values in the two final columns are the mean differences (Δ) between the velocity estimates from each line and the final velocity for each star.

Ion	λ [Å]	$\Delta_{\rm Night1}$ [km s^{-1}]	$\Delta_{\rm Night2}$ [km s^{-1}]
O-type ($\leq$ O4) stars:			
He II	4025.60	2.0 ± 10.8	-1.5 ± 9.3
He II	4199.83	-1.0 ± 6.6	3.2 ± 6.7
He II	4541.59	-1.0 ± 12.2	-1.7 ± 4.7
O-type (> O4) stars:			
He II	4199.83	-1.7 ± 12.4	-1.9 ± 9.0
He I	4387.93	0.4 ± 9.8	0.0 ± 8.4
He II	4541.59	1.8 ± 10.4	-0.2 ± 7.9
He II	4685.71	2.2 ± 10.7	2.0 ± 10.0
He I	4713.15	-1.6 ± 9.3	...
He I	4921.93	-1.2 ± 7.4	...
B-type stars (excl. B9):			
He I	4009.26	0.8 ± 8.8	1.8 ± 9.8
He I	4143.76	1.0 ± 7.1	1.1 ± 5.7
He I	4387.93	-2.1 ± 5.4	-2.6 ± 4.9
He I	4437.55	-0.1 ± 8.6	0.5 ± 9.2
Si III	4552.62	-1.2 ± 6.1	-1.1 ± 5.5
Si III	4567.84	-0.7 ± 5.2	2.1 ± 7.7
Si III	4574.76	-0.9 ± 7.3	-1.8 ± 7.0
He I	4713.15	2.4 ± 5.4	...
He I	4921.93	0.7 ± 6.3	...
B9/A-type stars:			
H	4101.73	-3.6 ± 5.2	-2.4 ± 1.8
Si II	4128.07	3.8 ± 11.0	4.5 ± 9.0
Si II	4130.89	-0.3 ± 3.2	0.9 ± 10.9
H	4340.47	-3.7 ± 3.3	-4.2 ± 7.6
He I	4471.48	2.3 ± 10.2	0.3 ± 5.0

Notes. Wavelengths are from the NIST atomic spectra database (Kramida et al. 2012).

These adopted lines were not available at the earliest and latest types in the AAOmega sample. Thus, for the earliest O-type stars ($\leq$O4) we used He II $\lambda\lambda$4026, 4200, 4542[4]. For the later-type (B9 and A-type) spectra we used Hδ and Hγ, combined with Si II $\lambda\lambda$4128-31 and He I λ4471.

Mean RVs for each target for the two nights, v_1 and v_2, are presented in Table 2. The quoted uncertainties are the standard errors (s.e.) on the means, and the sixth and eighth columns give the number of measured lines (n); mean values are only calculated for spectra where $n \geq 3$. As a check for systematics in our measurements (e.g. line blends) and the adopted rest wavelengths, for each line in our analysis we calculated the mean residuals ($\Delta_{\rm Night1}$ and $\Delta_{\rm Night2}$, and their standard deviations) compared to the estimated RV for each star; these are given in the third and fourth columns of Table 5. In general, there are no significant systematic offsets present in the adopted lines. The Balmer lines in the cooler spectra appear to yield (marginally) different RV estimates, but these values are sufficient for our purposes.

4.1. Binaries

Our observations were obtained on two (consecutive) nights so our velocity estimates are somewhat limited in the search for

[4] At such types λ4026 is strongly dominated by He II absorption.

variations arising from single-lined binaries. Nonetheless, we employed similar criteria to those used by Sana et al. (2013) and Dunstall et al. (2015) for identification of spectroscopic binaries from the VFTS. For stars with RV estimates from both nights, we consider it as a spectroscopic binary if they satisfy that $|v_1 - v_2| > 20\,\mathrm{km\,s^{-1}}$ between the observations and that $|v_1 - v_2| \,/\, \sqrt{\sigma_1^2 + \sigma_2^2} > 4.0$, i.e. such variations are statistically significant, following the approach taken by Sana et al. (2013). The choice of the RV threshold for binary detection is a trade-off between the number of false positives arising from the effects of pulsations (and other atmospheric variations) and detections of real RV shifts from binary motion, as discussed by Sana et al. (2013) and Dunstall et al. (2015).

Employing these criteria, the RV estimates for only one star, AAΩ 30 Dor 053 (classified as B0.5 Ib Nwk), is formally significant as a SB1 system; this remains the case using a lower threshold of $|v_1 - v_2| > 16\,\mathrm{km\,s^{-1}}$ (as used by Dunstall et al. 2015, in their analysis of early B-type stars). There are a further six stars[5] with $|v_1 - v_2| > 20\,\mathrm{km\,s^{-1}}$, but with sufficient uncertainties on their RV estimates that they do not satisfy the second criterion; for the purposes of the calculations in the next section we exclude these potential (though unconfirmed) RV variables.

In summary, eleven SB2 systems were found in our spectroscopy (with an additional SB2 candidate, AAΩ 30 Dor 173), one SB1 system (AAΩ 30 Dor 053), and six potential RV variables; these objects and their spectral classifications are listed in Table 6. Eight are known eclipsing systems from Graczyk et al. (2011) from the third phase of the Optical Gravitational Lensing Experiment (OGLE). Using a 2″ search radius we then cross-matched our remaining targets with the Graczyk et al. (2011) catalogue, finding eight other eclipsing systems that were undetected as binaries from the available spectra. The OGLE identifiers, periods, and light-curve classifications are included in Table 6. Similar cross-checks with the luminous variables in the LMC reported by Szczygieł et al. (2010) yielded only one match – AAΩ 30 Dor 286 (Sk−69°238), classified as O7.5 Ib(f), which was detected as a low-amplitude (∼0.25 mag) photometric variable.

4.2. Velocity Distributions and Radial-Velocity Outliers

We calculated mean velocities of all our targets with RV estimates, and for subsamples limited to the O- and BA-type spectra. The resulting means and their associated standard deviations are summarised in Table 7, and the systemic value is in good agreement with results from the VFTS (Evans et al. 2015). In calculation of these results we have excluded stars flagged as potential RV variables in the previous section and those identified as eclipsing binaries. We also identified and (by iteration) excluded RV outliers for both nights, defined as stars with: $|v - \overline{v}| > 3\sigma$.

The RV estimates of the nine outliers are summarised in Table 8. Both AAΩ 30 Dor 254 and 383 only have estimates (from three or more lines) for one night, but qualitative comparison of the spectra from the two nights reveals no obvious shifts; indeed, the former of these two objects is VFTS 016, identified as a runaway star by Evans et al. (2010, including analysis of these data).

For completeness, we note that two stars, AAΩ 30 Dor 248 and 282, are (marginal) outliers in the estimates from one of the nights, suggesting either small RV variations or simply that we are at the limit of the available data (given that relatively few lines were available for RV estimates for these stars). Following the suggestion by Walborn et al. (2002a) that Sk−68°137 and BI 253 (VFTS 072, AAΩ 30 Dor 276) might be massive runaways, the case of AAΩ 30 Dor 248 is similarly intriguing given its location (∼22′ NNW of R136, see Fig. 1). Indeed, if its OC-type classification does indicate an early evolutionary phase it raises the question of whether it is an ejected runaway, or formed more locally (in relative isolation given the apparent lack of a nearby star-forming region).

AAΩ 30 Dor 159 (W61 28-23) is the second largest outlier, and we note that Massey et al. (2005) reported a comparable RV (∼350 km s^{-1}, see their Fig. 9) from observations in 1999 January. Whether this is a genuine runaway, or just chance observations of similar RVs for a large-amplitude binary system will require further spectroscopic monitoring. Indeed, additional spectroscopy of each object in Table 8 will be required to ascertain their true status.

[5] For completeness: AAΩ 30 Dor 084, 085, 135, 160, 192, and 419.

Table 7. Mean radial velocities and dispersions for the AAΩ sample for both nights ($\overline{v_1}$ and $\overline{v_2}$, respectively), excluding known and candidate binaries (see Section 6) and stars with outlying velocities (Table 8).

Sample	$\overline{v_1} \pm$ s.d. [km s^{-1}]	n	$\overline{v_2} \pm$ s.d. [km s^{-1}]	n
All	274.1 ± 16.4	199	274.3 ± 16.5	194
O-type	275.1 ± 19.5	68	275.3 ± 18.6	61
BA-type	273.6 ± 14.6	131	273.8 ± 15.5	133

5. Summary

We have presented spectral classifications from optical spectroscopy with 2dF-AAOmega for 263 massive stars in the NE region of the LMC, together with RV estimates for 233 stars in the sample. Ten stars have classifications of O4 or earlier, with two (AAΩ 30 Dor 248 and 280) classified as OC-type given the nitrogen deficiency of their spectra combined with carbon emission; this is the first time such effects have been seen at such early types.

The spectra of 11 of our targets reveal them as SB2 systems, with a possible contribution from a secondary component seen in one other spectrum. From analysis of the RVs estimated from consecutive nights we identified one SB1 system and six candidate RV variables. Eight of these 19 objects are known eclipsing binaries from the OGLE survey (Graczyk et al. 2011). Eight of our other targets were also classified as eclipsing systems by Graczyk et al. (2011), but were undetected as binaries from our spectroscopy.

Using a 3σ threshold compared to the systemic velocity (and excluding the known and candidate binaries), the estimated RVs were used to identify nine RV outliers (Table 8). These are likely to be large-amplitude binaries or runaway stars, and follow-up spectroscopy is required to clarify their nature.

Acknowledgements. We are grateful to Nolan Walborn for his careful reading of the draft manuscript, and for his thoughts regarding the classification of the early-type spectra. We also thank the referee for their constructive comments, and Russell Cannon and Gary Da Costa for their help with the observations.

References

Bonanos, A. Z., Lennon, D. J., Köhlinger, F., et al. 2010, AJ, 140, 416
Bonanos, A. Z., Massa, D. L., Sewilo, M., et al. 2009, AJ, 138, 1003
Bosch, G., Terlevich, E., & Terlevich, R. 2009, AJ, 137, 3437
Bressert, E., Bastian, N., Evans, C. J., et al. 2012, A&A, 542, A49
Brunet, J. P., Imbert, M., Martin, N., et al. 1975, A&AS, 21, 109

Table 6. Summary of known binaries and candidate radial-velocity variables in the AAOmega sample.

Star	Spectral classification	AAΩ status	OGLE LMC-ECL	P_{OGLE} [d]	$Type_{OGLE}$
010	O9.5: + early B	SB2	...	...	...
021	B0.5: + early B	SB2	16629	2.923299	EC
024	B1.5 Ib Nwk	...	16646	26.225620	ED
027	B0.5: + early B	SB2	16675	3.748640	ED
038	B1-1.5 V-III	...	16881	3.167171	ED/VAR
053	B0.5 Ib Nwk	SB1	...	...	...
058	B1-1.5 V-III	...	17198	3.290830	ED
065	O9.2-9.5 V	...	17334	1.362346	ESD
084	B1.5 Ib Nwk	RV var?	17823	4.585031	EC
085	B0 V	RV var?	...	...	...
114	B0.2 III: + early B	SB2	...	...	...
122	O9.5 III + B0:	SB2	18794	5.946846	ED
130	B0.2: + early B	SB2	...	...	...
135	B1.5 III-II	RV var?	...	...	...
160	B1.5 V-III	RV var?	...	...	...
173	B0.5 Ib Nwk?	SB2?	19892	4.682925	ED
178	O6 V((f))	...	19996	1.079433	ED
192	O8.5 IIn	RV var?	...	...	...
267	O9.5: II + early B	SB2	20901	1.554470	ED
330	O9: V-III + O9.5: V-III	SB2	21568	3.225450	ED
337	O9: V-III + O9.7: V-III	SB2	...	...	...
352	Mid-O V	...	21844	100.374558	ED
371	O9.5 II	...	22166	1.759227	ED
374	Early B + early B	SB2	22270	5.414011	ED
381	O9 III	...	22429	100.032930	ED/VAR
414	O8.5 Iabf (+ OB?)	SB2	...	...	...
419	B1-1.5 I	RV var?	...	...	...

Notes. Details of eclipsing binaries known from the OGLE survey are from Graczyk et al. (2011); classifications of light-curve variability in the final column are: EC = contact eclipsing binary; ED = detached eclipsing binary; ESD = semi-detached eclipsing binary; ED/VAR = detached with additional variability superimposed. Classifications of the spectra for AAΩ 30 Dor 084 and 374 were given by Muraveva et al. (2014), identified in their Table A3 as lm0020n19615 and lm0031122987, respectively; the more detailed classifications given here now supercede those.

Table 8. Stars with outlying radial velocities, which are candidate large-amplitude binaries or runaway stars.

Star	Spectral type	$v_1 \pm$ s.d. [km s^{-1}]	$(v_1 - \overline{v_1})$ [km s^{-1}]	$\lvert v_1 - \overline{v_1}\rvert/\sigma$	$v_2 \pm$ s.d. [km s^{-1}]	$(v_2 - \overline{v_2})$ [km s^{-1}]	$\lvert v_2 - \overline{v_2}\rvert/\sigma$
097	O9 IIIn	209.0 ± 15.3	-65.1 ± 22.4	4.0	214.7 ± 9.5	-59.6 ± 19.1	3.6
159	O3.5 III(f*)	370.1 ± 5.7	96.0 ± 17.4	5.8	377.8 ± 7.2	103.5 ± 18.0	6.3
195	B1 Ib Nwk	328.3 ± 12.2	54.2 ± 20.4	3.3	329.9 ± 4.3	55.6 ± 17.1	3.4
254	O2 III-If*	...	...	...	190.3 ± 1.6	-84.0 ± 16.6	5.1
383	O9.2 Ib	189.0 ± 10.1	-85.1 ± 19.3	5.2	...	...	...
401	B0.5 Ia	222.5 ± 7.5	-51.6 ± 18.0	3.1	216.1 ± 7.1	-58.2 ± 18.0	3.5
424	B0.7 Ib Nwk	192.2 ± 10.2	-81.9 ± 19.3	5.0	199.9 ± 7.1	-74.4 ± 18.0	4.5
426	O6.5 III(f)	213.6 ± 14.5	-60.5 ± 21.9	3.7	220.7 ± 12.0	-53.6 ± 20.4	3.2
428	O7.5 V((f))	166.4 ± 5.8	-107.7 ± 17.4	6.6	163.7 ± 8.1	-110.6 ± 18.4	6.7

Notes. The adopted mean velocities ($\overline{v_1}$ and $\overline{v_2}$) are those from the first entry of Table 7 (which exclude the above stars and candidate binaries). AAΩ 30 Dor 254 = VFTS 016, the runaway star reported by Evans et al. (2010).

Conti, P. S., Garmany, C. D., & Massey, P. 1986, AJ, AJ, 92
Dunstall, P. R., Dufton, P. L., Sana, H., et al. 2015, A&A, 580, A93
Evans, C., Hunter, I., Smartt, S., et al. 2008, Msngr, 131, 25
Evans, C. J., Hainich, R., Oskinova, L. M., et al. 2012, ApJ, 753, 173
Evans, C. J. & Howarth, I. D. 2008, MNRAS, 386, 826
Evans, C. J., Howarth, I. D., Irwin, M. J., Burnley, A. W., & Harries, T. J. 2004, MNRAS, 353, 601
Evans, C. J., Kennedy, M., Dufton, P. L., et al. 2015, A&A, 574, A13
Evans, C. J., Lennon, D. J., Smartt, S. J., & Trundle, C. 2006, A&A, 456, 623
Evans, C. J., Taylor, W. D., Hénault-Brunet, V., et al. 2011, A&A, 530, A108
Evans, C. J., Walborn, N. R., Crowther, P. A., et al. 2010, ApJ, 715, L74
Fariña, C., Bosch, G. L., Morrell, N., Barbá, R., & Walborn, N. R. 2009, AJ, 138, 510
Fitzpatrick, E. L. 1988, ApJ, 335, 703
Fitzpatrick, E. L. 1991, PASP, 103, 1123
Graczyk, D., Soszyński, I., Poleski, R., et al. 2011, AcA, 61, 103
Grindlay, J., Tang, S., Los, E., & Servillat, M. 2012, in IAU Symposium 285: Opening the 100-Year Window for Time-Domain Astronomy, ed. E. Griffin, R. Hanisch, & R. Seaman, Vol. 285, 29
Hamann, W.-R. & Gräfener, G. 2003, A&A, 410, 990
Hamann, W.-R. & Gräfener, G. 2004, A&A, 427, 697
Hénault-Brunet, V., Evans, C. J., Sana, H., et al. 2012a, A&A, 546, A73

Hénault-Brunet, V., Gieles, M., Evans, C. J., et al. 2012b, A&A, 545, L1
Henize, K. 1956, ApJS, 2, 315
Jaxon, E. G., Guerrero, M. A., Howk, J. C., et al. 2001, PASP, 113, 1130
Kramida, A., Ralchenko, Y., & Reader, J. and NIST ASD Team. 2012, in NIST Atomic Spectra Database (v5.0); http:/physics.nist.gov/asd (National Institute of Standards and Technology, Gaithersburg, MD.)
Lamb, J. B., Oey, M. S., Graus, A. S., Adams, F. C., & Segura-Cox, D. M. 2013, ApJ, 763, 101
Lamb, J. B., Oey, M. S., Werk, J. K., & Ingleby, L. D. 2010, ApJ, 725, 1886
Lewis, I. J., Cannon, R. D., Taylor, K., et al. 2002, MNRAS, 333, 279
Lucke, P. B. & Hodge, P. W. 1970, AJ, 75, 171
Massey, P. 2002, ApJS, 141, 81
Massey, P., Lang, C. C., DeGioia-Eastwood, K., & Garmany, C. 1995, ApJ, 438, 188
Massey, P., Morrell, N. I., Neugent, K. F., et al. 2012, ApJ, 748, 96
Massey, P. & Olsen, K. A. G. 2003, AJ, 126, 2867
Massey, P., Puls, J., Pauldrach, A. W. A., et al. 2005, ApJ, 627, 477
Massey, P., Waterhouse, E., & DeGioia-Eastwood, K. 2000, AJ, 119, 2214
Melnick, J. 1985, A&A, 153, 235
Muraveva, T., Clementini, G., Maceroni, C., et al. 2014, MNRAS, 443, 432
Oey, M. S. 1996a, ApJS, 104, 71
Oey, M. S. 1996b, ApJS, 465, 231
Oey, M. S., Lamb, J. B., Kushner, C. T., Pellegrini, E. W., & Graus, A. S. 2013, ApJ, 768, 66
Oskinova, O., Hamann, W.-R., & Feldmeier, A. 2007, A&A, 476, 1331
Parker, J. W. 1993, AJ, 106, 560
Pietrzyński, G., Graczyk, D., Gieren, W., et al. 2013, Nature, 495, 76
Pojmański, G. 2002, AcA, 52, 397
Rivero González, J. G., Puls, J., Massey, P., & Najarro, F. 2012, A&A, 543, A95
Sana, H., de Koter, A., de Mink, S. E., et al. 2013, A&A, 550
Sanduleak, N. 1969, Contrib. Cerro Tololo Inter-American Obs., No. 89
Saunders, W., Bridges, T., Gillingham, P., et al. 2004, in Ground-based Instrumentation for Astronomy, ed. A. Moorwood & M. Iye, Vol. 5492 (Proc. SPIE), 389
Schild, H. & Testor, G. 1992, A&AS, 92, 729
Sharp, R., Saunders, W., Smith, G., et al. 2006, in Ground-based and Airborne Instrumentation for Astronomy, ed. I. McLean & M. Iye, Vol. 6269 (Proc. SPIE), 0G
Sota, A., Maíz Apellániz, J., Morrell, N. I., et al. 2014, ApJS, 211, 10
Sota, A., Maíz Apellániz, J., Walborn, N. R., et al. 2011, ApJS, 193, 24
Stock, J., Osborn, W., & Ibañez, M. 1976, A&AS, 24, 35
Szczygieł, D. M., Stanek, K. Z., Bonanos, A. Z., et al. 2010, AJ, 140, 14
Testor, G. & Niemela, V. 1998, A&AS, 130, 527
van Loon, J. T., Bailey, M., Tatton, B. L., et al. 2013, A&A, 550, A108
Walborn, N. R. 1972, AJ, 77, 312
Walborn, N. R. 1973, AJ, 78, 1067
Walborn, N. R. 1976, ApJ, 205, 419
Walborn, N. R. & Blades, J. C. 1997, ApJS, 112, 457
Walborn, N. R. & Fitzpatrick, E. L. 1990, PASP, 102, 379
Walborn, N. R., Howarth, I. D., Evans, C. J., et al. 2010, AJ, 139, 1283
Walborn, N. R., Howarth, I. D., Lennon, D. J., et al. 2002a, AJ, 123, 2754
Walborn, N. R., Lennon, D. J., Haser, S., Kudritzki, R. P., & Voels, S. A. 1995, PASP, 107, 104
Walborn, N. R., Maíz Apellániz, J., & Barbá, R. 2002b, AJ, 124, 1601
Walborn, N. R., Morrell, N. I., Howarth, I. D., et al. 2004, ApJ, 608, 1028
Walborn, N. R., Sana, H., Simón-Díaz, S., et al. 2014, A&A, 564, A40
Wang, L. 1992, Msngr, 69, 34
Welty, D. E., Federman, S. R., Gredel, R., Thorburn, J. A., & Lambert, D. L. 2006, ApJS, 165, 138
Westerlund, B. E. 1961, Uppsala Astron. Obs. Ann., 5, 1
Zaritsky, D., Harris, J., Thompson, I. B., & Grebel, E. K. 2004, AJ, 128, 1606

Table 2. Observational parameters of target stars.

Star	α (J2000)	δ (J2000)	Spectral type	$v_1 \pm$ s.e. [km s^{-1}]	n	$v_2 \pm$ s.e. [km s^{-1}]	n	Comments
001	05 27 33.34	−69 01 22.0	O9.7 II-Ib	267.0 ± 2.7	6	265.5 ± 3.3	3	
004	05 27 38.31	−69 08 29.9	B1 Iab Nwk	279.8 ± 6.0	6	277.1 ± 4.4	6	
008	05 27 54.14	−68 59 27.1	B0:	...	...	...	...	
009	05 27 56.22	−69 07 21.8	B0.7 II	284.6 ± 2.7	3	...	...	
010	05 27 57.98	−68 53 11.9	O9.5: + early B	Binary (SB2)				
011	05 27 58.44	−68 58 33.1	B1.5 Ib Nwk	272.8 ± 0.7	9	276.3 ± 2.6	7	
014	05 28 02.57	−69 13 49.5	O9.7 Iab	239.2 ± 7.3	6	...	...	Sk−69°144
015	05 28 06.98	−68 56 44.4	B2 Ib	279.7 ± 1.5	9	278.4 ± 2.7	7	Sk−68°91a
016	05 28 10.27	−68 49 42.6	B9 Ib	282.5 ± 1.2	4	282.3 ± 1.4	5	
017	05 28 11.20	−69 09 14.5	B0.7 II-Ib	275.1 ± 2.5	9	269.2 ± 2.6	7	
018	05 28 12.60	−69 03 14.7	B0.5 Ib Nwk?	272.3 ± 3.0	8	278.3 ± 5.5	7	
019	05 28 13.47	−69 13 29.0	B1 Ia Nstr	285.7 ± 1.5	9	284.9 ± 2.1	7	
020	05 28 18.79	−69 15 19.8	O9.5 III(n)	273.6 ± 6.7	6	...	...	Sk−69°146
021	05 28 19.07	−69 04 52.6	B0.5: + early B	Binary (SB2)				
024	05 28 21.06	−68 47 37.3	B1.5 Ib Nwk	274.8 ± 1.4	9	287.9 ± 2.3	7	
025	05 28 21.40	−69 10 14.4	B1 Ib	281.6 ± 2.6	9	278.0 ± 1.8	7	
026	05 28 23.55	−68 58 43.6	B2 Ib	278.8 ± 0.8	9	280.7 ± 3.9	7	
027	05 28 24.06	−69 12 26.2	B0.5: + early B	Binary (SB2)				
028	05 28 26.29	−68 52 07.5	B2.5 Ib	281.4 ± 1.9	9	281.5 ± 1.3	7	
030	05 28 31.13	−69 08 06.1	B1.5 III-II(n)	266.6 ± 10.8	4	273.4 ± 6.7	4	
033	05 28 36.18	−69 28 47.1	B5 Ib	274.5 ± 4.0	5	268.7 ± 2.5	3	
034	05 28 36.93	−68 50 03.1	B0.7 Ib(n) Nwk	285.2 ± 6.1	5	282.1 ± 3.4	5	LH 64-6
036	05 28 45.65	−68 49 31.4	B1.5 II-Ib(n)	...	...	272.9 ± 5.5	5	W61 16-6; LH 64-7
038	05 28 46.46	−68 46 15.8	B1-1.5 V-III	...	...	...	...	W61 16-7; LH 64-33
040	05 28 46.97	−68 47 47.9	ON2 III(f*)	273.0 ± 4.1	3	280.2 ± 5.3	5	W61 16-8; LH 64-16
042	05 28 52.80	−69 00 53.9	B0.7 II-Ib	286.4 ± 1.8	7	288.9 ± 4.3	7	
043	05 28 57.68	−68 47 20.4	B1 Ib(n) Nwk	282.5 ± 2.8	4	288.6 ± 2.2	4	W61 16-29 (in LH 64)
045	05 29 01.92	−69 22 50.6	B1-2e	255.4 ± 3.1	5	265.8 ± 3.5	4	
047	05 29 03.22	−69 24 39.8	B9 Ib	287.2 ± 4.2	4	288.2 ± 1.6	4	SOI 624
049	05 29 04.89	−69 29 52.4	A5 II	...	...	300.0 ± 9.6	3	SOI 625
050	05 29 11.90	−68 44 58.8	B1 Ib Nwk	274.9 ± 1.6	9	275.7 ± 2.0	7	W61 16-62; LH 64-60
053	05 29 14.27	−68 42 01.2	B0.5 Ib Nwk	312.1 ± 3.7	7	256.8 ± 3.2	6	
054	05 29 20.84	−68 44 52.9	B0-0.5e	...	...	...	...	W61 16-78; LH 64-63
055	05 29 21.20	−69 09 57.3	B3 Iab	277.7 ± 1.6	9	274.8 ± 1.9	5	
056	05 29 22.46	−69 30 22.7	B1.5 Ib(n)	284.8 ± 2.1	5	291.4 ± 6.8	4	
057	05 29 23.21	−68 47 11.0	O8 III(n)((f))	300.6 ± 5.4	6	...	...	LH 64-4
058	05 29 24.59	−68 42 12.7	B1-1.5 V-III	249.9 ± 3.4	3	...	...	
059	05 29 28.58	−69 02 50.5	B0.5-0.7 V-III	...	...	293.8 ± 11.6	3	
060	05 29 28.68	−69 23 31.8	B1 Ia	257.6 ± 1.3	9	252.4 ± 2.4	7	Sk−69°157
061	05 29 30.51	−69 07 12.5	B1.5 Ib Nwk	282.6 ± 2.6	9	282.7 ± 3.6	6	
062	05 29 31.46	−69 04 20.2	B1.5 III-II	258.1 ± 1.5	7	251.1 ± 4.5	7	
063	05 29 33.59	−69 13 04.7	B1.5 Ib Nwk	275.0 ± 1.2	9	276.0 ± 0.9	7	
064	05 29 35.76	−68 46 23.8	B1 Iab Nstr	285.2 ± 1.3	9	286.1 ± 1.8	7	LH 64-39
065	05 29 43.21	−68 45 41.2	O9.2-9.5 V	260.8 ± 4.0	5	265.5 ± 5.4	3	
068	05 29 51.01	−69 24 31.7	B3 Ib	272.3 ± 3.3	9	269.9 ± 1.5	7	
069	05 29 52.68	−69 00 02.6	B1 II	259.3 ± 1.5	9	273.8 ± 2.4	7	
071	05 29 54.41	−69 05 19.0	B3 Ib	270.7 ± 2.5	7	275.1 ± 1.0	4	
072	05 30 05.14	−69 13 47.7	B1.5 II-Ib	280.8 ± 3.8	8	295.2 ± 3.4	5	

continued on next page

Table 2. *continued*

Star	α (J2000)	δ (J2000)	Spectral type	$v_1 \pm$ s.e. [km s^{-1}]	n	$v_2 \pm$ s.e. [km s^{-1}]	n	Comments
074	05 30 08.99	−68 48 36.6	O9.7 Iab	289.3 ± 3.9	6	288.4 ± 3.3	3	Sk−68°105
075	05 30 10.75	−68 41 15.4	B0.5: V-III	296.4 ± 16.3	3	...	...	
076	05 30 16.90	−69 08 06.0	B1 Ib	301.3 ± 2.7	8	307.6 ± 2.6	7	
077	05 30 16.93	−69 26 09.3	B0.2 Ib	282.1 ± 3.3	8	281.2 ± 2.6	6	
078	05 30 21.47	−68 53 30.1	B3 Iab	288.0 ± 1.0	8	288.4 ± 2.3	7	SOI 399
079	05 30 29.13	−69 03 25.8	B0 III	273.4 ± 1.9	8	275.9 ± 2.0	7	
082	05 30 36.99	−69 32 21.4	B9 Ib	295.2 ± 3.6	4	297.3 ± 5.1	4	
083	05 30 37.24	−69 15 06.4	B1.5 Ia Nstr	280.9 ± 1.2	9	275.2 ± 1.1	7	Sk−69°167
084	05 30 41.93	−69 19 27.9	B1.5 Ib Nwk	330.8 ± 3.1	8	306.0 ± 3.1	7	
085	05 30 53.95	−69 03 29.7	B0 V	310.9 ± 3.3	5	272.9 ± 3.3	7	
086	05 30 55.71	−69 21 48.3	B1.5 Ib	272.5 ± 1.2	9	272.7 ± 2.6	7	
089	05 30 58.94	−69 14 02.9	B1-1.5 Ib(n)	269.0 ± 2.0	4	265.4 ± 4.0	5	
090	05 30 59.11	−68 47 45.3	AF (A0kF5)	...	...	...	...	
091	05 30 59.28	−69 09 48.6	B2.5 Ib(n)	277.8 ± 3.5	7	285.5 ± 4.3	5	
092	05 30 59.77	−69 16 56.9	B1 Iab	281.5 ± 1.6	8	286.1 ± 2.6	7	
093	05 31 19.23	−69 18 13.8	B1 Ib Nwk	291.7 ± 1.1	8	290.0 ± 2.9	7	
094	05 31 21.29	−69 16 00.9	B1 Iab Nstr?	282.9 ± 1.9	9	288.6 ± 3.2	6	
095	05 31 21.38	−69 20 34.5	B9 Ib	274.4 ± 2.9	4	277.0 ± 2.3	4	
096	05 31 21.95	−69 19 15.3	B1 II	279.9 ± 3.6	5	286.1 ± 8.6	5	
097	05 31 34.00	−68 50 46.7	O9 IIIn	209.0 ± 7.7	4	214.7 ± 4.7	4	
098	05 31 35.25	−69 30 47.7	B5 Iab	269.9 ± 1.5	9	271.7 ± 1.8	7	Sk−69°176
099	05 31 37.74	−69 28 25.5	B2 Ib	274.4 ± 1.4	8	270.5 ± 2.5	7	
100	05 31 47.34	−69 12 44.3	B0.7 II	275.1 ± 1.6	7	260.1 ± 6.9	4	
101	05 31 47.38	−68 30 19.3	O2-3 V((f*)) + OB	309.3 ± 12.2	3	293.5 ± 4.1	3	
103	05 31 48.26	−69 14 21.6	B1 Ia	283.4 ± 1.6	9	290.2 ± 2.4	7	
104	05 31 51.87	−68 51 40.1	B1.5 Ib	272.6 ± 1.2	9	275.4 ± 1.3	7	
105	05 31 53.96	−69 33 30.1	O9.2 II	310.2 ± 5.7	6	307.1 ± 3.1	4	Sk−69°178
106	05 31 55.46	−68 40 08.4	O6.5 V((f))	269.9 ± 8.0	6	288.1 ± 6.8	3	D226-5 (Oey 1996a)
109	05 32 06.65	−69 26 56.9	B1 Ia	273.0 ± 1.0	8	274.9 ± 2.2	6	Sk−69°180
110	05 32 07.32	−69 14 36.5	B1.5 II	284.7 ± 5.8	5	278.8 ± 3.9	7	
111	05 32 21.29	−69 08 28.0	B1 Ib Nwk	294.1 ± 1.5	9	298.3 ± 3.2	7	
112	05 32 25.90	−68 55 15.9	B1 Iab Nstr	264.5 ± 1.3	9	266.7 ± 1.7	7	Sk−68°117
113	05 32 27.89	−68 49 38.4	O9.7 Iab	320.8 ± 3.5	5	322.6 ± 6.0	4	Sk−68°118
114	05 32 29.49	−69 24 48.4	B0.2 III: + early B	Binary SB2				
115	05 32 30.82	−69 24 11.2	B1 Ib-Iab Nwk?	278.1 ± 6.2	6	282.1 ± 4.3	3	
116	05 32 33.86	−69 14 25.2	B1.5 Ib Nwk	278.7 ± 1.7	9	280.7 ± 4.0	7	
117	05 32 36.34	−69 05 41.1	B0.7 Ib Nwk	262.5 ± 1.9	8	269.2 ± 3.0	7	
120	05 32 41.76	−68 54 17.4	O9-9.2 III-II(n)	305.9 ± 5.7	5	306.2 ± 5.1	4	Sk−68°119
121	05 32 42.51	−69 29 21.9	B1 Ib	281.0 ± 1.6	9	280.4 ± 1.9	7	
122	05 32 47.88	−68 37 26.1	O9.5 III + B0:	Binary (SB2)				Sk−68°120
123	05 32 57.48	−69 02 15.5	B0.7 II	247.7 ± 2.9	9	242.5 ± 4.3	7	
124	05 33 05.67	−69 23 09.1	B0.2 III(n)	...	...	254.8 ± 0.3	3	
125	05 33 05.70	−69 18 39.9	B0.2 III	291.6 ± 3.6	7	296.6 ± 1.9	6	
126	05 33 08.37	−69 10 37.8	B8 Iab	270.3 ± 2.5	5	268.5 ± 4.4	4	
127	05 33 09.36	−68 28 39.6	O9 III	256.4 ± 2.3	6	255.8 ± 0.7	4	
128	05 33 16.95	−69 57 11.2	B5 Ib(n)	292.6 ± 17.3	3	...	...	
129	05 33 19.13	−68 43 28.8	B0 Iab	258.6 ± 3.1	7	259.0 ± 0.9	6	
130	05 33 19.26	−69 14 26.0	B0.2: + early B	Binary (SB2)				
132	05 33 23.37	−69 16 50.3	B0.7 Ib	273.9 ± 1.2	9	277.3 ± 2.5	7	

continued on next page

Table 2. *continued*

Star	α (J2000)	δ (J2000)	Spectral type	$v_1 \pm$ s.e. [km s^{-1}]	n	$v_2 \pm$ s.e. [km s^{-1}]	n	Comments
133	05 33 26.37	−69 19 27.6	B5 Ib	271.4 ± 2.0	6	272.3 ± 3.4	5	
134	05 33 30.08	−68 43 52.0	O9.5 IIIn	289.6 ± 7.9	4	296.6 ± 7.6	3	
135	05 33 31.56	−69 22 44.6	B1.5 III-II	271.6 ± 3.0	7	248.6 ± 2.7	6	
136	05 33 31.71	−69 18 28.6	B0 Ia	238.1 ± 2.5	8	244.6 ± 1.9	5	Sk−69°184
137	05 33 39.26	−69 06 47.1	B5 Iab	277.9 ± 2.4	6	274.3 ± 2.1	6	
138	05 33 42.59	−69 26 36.8	B1 Ia	270.4 ± 2.5	8	277.7 ± 3.8	6	Sk−69°186
139	05 33 45.32	−69 17 59.3	B0.7 II(n) Nwk	279.3 ± 5.9	4	283.5 ± 8.4	5	
140	05 33 58.03	−68 42 29.8	O6.5 II(f)	280.5 ± 3.1	6	...	...	
142	05 34 06.32	−69 25 09.0	O6.5(n)(f)p	...	...	...	...	BI 214
143	05 34 06.35	−69 10 41.1	B1 Ib Nstr?	287.9 ± 1.5	8	291.8 ± 2.6	7	
144	05 34 09.25	−69 28 28.2	O9 II	257.0 ± 5.6	6	264.6 ± 6.3	4	
145	05 34 09.80	−69 38 44.6	O9 III(n)	285.1 ± 4.8	6	285.7 ± 2.5	4	
146	05 34 16.44	−68 53 58.3	O9.5 III	286.0 ± 2.8	6	279.9 ± 3.3	4	
149	05 34 33.17	−69 01 09.5	O9.5 III	314.9 ± 3.2	6	304.3 ± 2.2	5	
150	05 34 37.32	−69 41 17.7	O6 V((f))z	285.5 ± 3.1	6	292.5 ± 6.5	4	
151	05 34 41.01	−69 44 54.1	O9.7 V	286.6 ± 4.2	6	294.3 ± 6.9	3	LH 81-1018
152	05 34 41.55	−69 28 58.0	B1.5 Ia	282.6 ± 1.6	9	280.1 ± 1.1	7	
155	05 34 43.86	−68 36 28.7	O9.7 II(n)	241.7 ± 7.7	5	...	...	BI 220
157	05 34 45.24	−69 27 14.9	O9.5 III-II	269.9 ± 3.1	6	265.7 ± 1.7	4	
159	05 34 50.16	−69 46 32.2	O3.5 III(f*)	370.1 ± 3.3	3	377.8 ± 4.1	3	W61 28-23 (in LH 81)
160	05 34 51.44	−69 28 48.2	B1.5 V-III	288.8 ± 10.8	3	267.7 ± 3.3	3	
161	05 34 51.89	−69 22 44.3	B2.5 Ib	273.2 ± 1.0	9	278.3 ± 1.3	7	BI 217
162	05 34 52.49	−69 25 50.6	B1 Ib	271.7 ± 0.8	9	271.2 ± 2.6	7	
163	05 34 53.74	−69 14 02.6	O5 III(f)	294.6 ± 8.5	3	307.1 ± 8.6	3	Sk−69°195
164	05 34 54.88	−69 38 29.5	B0 Ia$^+$	296.4 ± 1.7	8	301.1 ± 2.2	6	Sk−69°196
168	05 35 06.17	−69 19 47.3	B2.5 III	271.0 ± 3.1	5	267.0 ± 4.2	4	
169	05 35 10.99	−69 29 35.0	O9.2 V	283.3 ± 3.3	5	278.9 ± 4.1	3	
170	05 35 12.50	−68 51 13.4	B0.2 III(n)	284.0 ± 4.2	4	293.0 ± 8.4	5	W61 27-1 (in LH 85)
172	05 35 16.18	−68 58 17.9	B0.2 III	261.0 ± 3.2	5	277.1 ± 2.9	6	LH 89-7
173	05 35 19.37	−69 43 08.6	B0.5 Ib Nwk?	Binary (SB2?)				
174	05 35 22.88	−69 27 07.4	B0 III	273.6 ± 2.6	9	267.1 ± 3.3	7	
176	05 35 24.46	−69 18 07.6	B1 II-Ib	281.3 ± 1.1	8	286.5 ± 1.1	7	
177	05 35 27.55	−69 41 22.2	B0.5 III	274.3 ± 2.8	6	279.0 ± 2.2	7	
178	05 35 34.18	−69 39 47.8	O6 V((f))	273.6 ± 1.8	3	272.0 ± 1.6	3	
179	05 35 37.36	−68 58 56.1	B0.2 III(n)	...	...	...	...	ST92 3-08 (in LH 89)
180	05 35 37.40	−68 51 42.6	B1 Iab Nwk	288.2 ± 2.4	9	292.2 ± 4.0	6	
181	05 35 38.69	−69 41 48.7	O3 If*	287.6 ± 5.0	3	280.8 ± 3.6	3	
182	05 35 40.31	−69 18 58.2	B1 Ib Nwk	288.6 ± 2.5	9	285.4 ± 0.7	7	
183	05 35 41.18	−69 28 48.1	B1.5 Ia Nstr	276.1 ± 1.2	9	275.5 ± 1.4	7	Sk−69°208
184	05 35 41.58	−69 24 57.6	B1 Ib Nwk	264.7 ± 2.5	7	269.1 ± 2.7	6	
185	05 35 46.46	−69 39 28.7	O9.2 III(n)	279.7 ± 6.8	5	285.9 ± 7.2	3	
186	05 35 49.80	−68 57 15.0	O7 III((f))	299.2 ± 4.5	5	299.4 ± 4.8	4	LH 89-62
187	05 35 51.92	−69 23 19.0	O6n(f)p	...	...	...	...	
189	05 35 55.29	−69 30 37.5	B1 Ia$^+$	250.4 ± 1.0	9	258.3 ± 2.1	6	Sk−69°209
190	05 35 55.74	−69 09 51.0	B0.5-1 Ia	303.7 ± 3.6	7	309.9 ± 9.5	5	
192	05 36 00.80	−69 27 34.9	O8.5 IIn	259.0 ± 10.9	6	279.8 ± 6.2	4	
194	05 36 06.65	−69 29 18.6	B0 Ia	254.4 ± 2.7	9	253.6 ± 7.6	6	
195	05 36 06.66	−68 57 54.5	B1 Ib Nwk	328.3 ± 4.1	9	329.9 ± 1.8	6	W61 27-31; LH 89-68; ST92 3-62

continued on next page

Table 2. *continued*

Star	α (J2000)	δ (J2000)	Spectral type	$v_1 \pm$ s.e. [km s^{-1}]	n	$v_2 \pm$ s.e. [km s^{-1}]	n	Comments
196	05 36 07.71	−69 15 57.9	O5 V((f))z	263.4 ± 0.7	3	258.0 ± 3.1	3	
197	05 36 08.02	−69 39 53.6	O9.5 III	279.9 ± 6.5	4	261.8 ± 14.2	3	
199	05 36 10.16	−68 54 56.4	B1.5 Ib Nwk	296.2 ± 1.8	9	297.0 ± 1.4	6	LH 89-96
200	05 36 12.98	−68 28 24.9	B0.7 Ib	283.4 ± 1.5	9	282.9 ± 2.7	6	Sk−68°127
201	05 36 13.43	−68 55 44.1	O9.7-B0 II	261.9 ± 4.0	5	...	...	W61 27-41
206	05 36 19.56	−69 23 38.6	B0 III	...	...	253.3 ± 8.0	3	
207	05 36 23.86	−69 26 08.3	B0.2 III(n)	...	...	...	...	
208	05 36 25.64	−69 29 15.9	O9 IV	245.4 ± 4.8	6	243.7 ± 3.0	4	
214	05 36 30.72	−69 48 54.9	O6.5 III(f)	243.9 ± 3.8	6	248.9 ± 6.9	4	Sk−69°216a
217	05 36 34.01	−69 22 28.1	O9 II	275.2 ± 7.0	6	272.2 ± 8.0	4	
218	05 36 35.50	−69 29 54.7	O9 V	279.3 ± 0.8	6	263.3 ± 4.9	4	
222	05 36 38.92	−69 27 58.8	O7.5 Iaf	270.2 ± 3.7	5	262.7 ± 2.2	3	
226	05 36 40.56	−69 22 56.9	O7.5 V((f))	244.6 ± 1.8	6	244.4 ± 0.7	4	
228	05 36 42.88	−69 24 49.9	O9.7-B0 V-III(n)	285.4 ± 5.6	4	292.4 ± 11.6	3	
229	05 36 44.28	−69 22 35.4	B0.2 Ia	260.6 ± 1.1	6	257.2 ± 1.2	4	
232	05 36 48.02	−69 29 55.7	O9.2 III	274.8 ± 3.4	6	272.4 ± 1.9	4	
233	05 36 48.68	−69 27 30.9	B0 Ib	268.0 ± 1.4	9	268.7 ± 1.6	6	
235	05 36 49.19	−69 25 51.8	O9.5 III	269.5 ± 0.8	5	262.3 ± 1.4	4	
236	05 36 49.28	−69 23 04.2	B0.5 Ib Nwk	245.8 ± 4.1	7	239.4 ± 7.7	5	
237	05 36 50.07	−69 11 51.1	O7.5 III	277.4 ± 1.9	5	284.2 ± 3.9	3	
239	05 36 50.22	−68 57 40.5	A3 Ib	272.0 ± 4.6	3	274.7 ± 3.5	4	
241	05 36 52.66	−68 22 08.8	B0 III(n)	243.9 ± 15.5	3	247.6 ± 14.9	3	Sk−68°132
248	05 37 01.34	−68 46 06.2	OC3.5 III(f*)	230.4 ± 9.1	3	218.5 ± 2.0	3	Sk−68°133
250	05 37 01.92	−69 30 00.1	B1.5 II	282.8 ± 1.8	9	269.3 ± 1.5	6	
252	05 37 06.53	−69 22 29.6	B0.5 II(n)	...	...	...	...	
254	05 37 08.98	−69 07 20.4	O2 III-If*	...	...	190.3 ± 0.9	3	VFTS 016
256	05 37 13.21	−69 25 30.6	B0.5 Ia Nwk	277.7 ± 1.6	9	271.8 ± 1.4	5	
257	05 37 13.55	−69 26 57.7	O9.7 II-Ib	282.0 ± 7.8	4	274.9 ± 16.4	3	
258	05 37 14.70	−69 23 28.8	O9.5 III(n)	281.8 ± 9.3	3	...	...	
260	05 37 17.92	−69 19 52.2	B0.7 II	304.5 ± 3.4	7	...	...	
261	05 37 20.22	−69 25 19.6	B0.5 II	265.9 ± 3.4	8	280.5 ± 5.9	5	
264	05 37 27.67	−68 56 58.8	O8.5 III(n)	237.2 ± 4.4	6	233.3 ± 3.4	4	BI 251
266	05 37 29.07	−68 45 39.2	B0.5 II-Ib	278.8 ± 3.0	6	277.2 ± 4.1	4	
267	05 37 29.09	−69 23 33.8	O9.5: II + early B	Binary (SB2)				
271	05 37 29.68	−69 14 51.8	O5.5 Iaf	...	...	...	...	
272	05 37 29.72	−69 27 41.1	O9.5 Ia	260.2 ± 4.2	6	253.7 ± 2.5	3	
273	05 37 29.93	−69 22 02.0	B1.5 Ib Nwk	284.3 ± 0.6	8	266.9 ± 1.6	7	
274	05 37 31.35	−69 42 23.4	B1 Iab Nstr?	241.1 ± 1.3	9	241.0 ± 0.8	6	Sk−69°232
275	05 37 33.73	−69 22 48.0	O7 V((f))	266.1 ± 1.8	6	262.6 ± 0.9	3	
276	05 37 34.45	−69 01 10.0	O2 V-III(n)((f*))	...	...	...	...	BI 253; VFTS 072
277	05 37 36.20	−68 50 56.1	B1 Ib-Iab(n) Nwk?	293.6 ± 3.8	4	293.8 ± 6.2	3	Sk−68°134
280	05 37 47.47	−69 18 30.5	O2-3 V-III((f*))	279.7 ± 1.8	3	276.1 ± 2.3	3	
281	05 37 48.18	−69 20 56.7	B1 Ib Nwk	300.9 ± 1.6	9	298.6 ± 3.2	5	
282	05 37 48.68	−69 28 19.9	O9 II	325.9 ± 4.3	6	314.7 ± 4.9	4	
283	05 37 50.03	−69 09 59.8	O7-8 III((f))	270.9 ± 1.4	5	282.4 ± 6.2	3	ST92 1-72; VFTS 171
284	05 37 57.89	−69 17 52.7	O8.5 II((f))	265.3 ± 3.7	6	268.8 ± 1.5	4	
285	05 37 57.96	−69 25 54.3	O9.7-B0 Ib-Iab	316.4 ± 1.6	4	314.7 ± 6.1	4	
286	05 37 59.18	−69 27 12.2	O7.5 Ib(f)	273.8 ± 5.9	5	269.6 ± 5.9	3	Sk−69°238
287	05 38 01.27	−69 22 13.9	B1 Ia Nstr	264.0 ± 1.6	9	269.6 ± 2.3	6	Sk−69°237

continued on next page

Table 2. *continued*

Star	α (J2000)	δ (J2000)	Spectral type	$v_1 \pm$ s.e. [km s^{-1}]	n	$v_2 \pm$ s.e. [km s^{-1}]	n	Comments
288	05 38 03.80	−69 20 14.7	O8.5-9 III	268.9 ± 2.7	6	273.6 ± 4.2	4	
290	05 38 17.51	−69 21 02.9	B0.7 Ib Nwk	250.5 ± 8.3	6	238.7 ± 3.6	4	
291	05 38 18.02	−69 19 24.4	O9.7 II	265.1 ± 5.0	5	...	...	
296	05 38 32.76	−69 04 32.8	O9 III(n)	...	...	...	...	P93-304/VFTS 389
308	05 38 40.16	−69 01 12.0	O8.5-9 II	257.7 ± 12.9	4	269.4 ± 3.3	4	P93-9017/VFTS 481
315	05 38 43.71	−69 21 27.0	B0 Iab	...	...	...	...	
318	05 38 44.26	−69 30 17.6	O8 Ib(f)	262.0 ± 3.9	5	277.1 ± 3.8	4	ST92 5-85
320	05 38 45.98	−69 28 36.9	O7n(f)p	...	...	...	...	ST92 5-82
324	05 38 48.07	−68 29 31.4	O9.7-B0 III	271.5 ± 3.1	5	...	...	Sk−68°139
330	05 38 58.05	−69 30 11.1	O9: V-III + O9.5: V-III	Binary (SB2)				W61 3-9; ST92 5-67
333	05 39 11.60	−69 30 37.3	O2-3(n)f*p Nwk	267.5 ± 8.6	3	254.0 ± 11.7	3	ST92 5-31
334	05 39 13.88	−69 29 49.7	O5-6 V((f))z	273.3 ± 5.4	3	281.1 ± 4.7	3	ST92 5-25
337	05 39 17.00	−69 23 46.6	O9: V-III + O9.7: V-III	Binary (SB2)				
338	05 39 17.94	−69 33 24.3	O7 V((f))	286.5 ± 6.8	5	294.4 ± 1.6	3	
339	05 39 25.84	−69 22 44.9	B0.2 Ib	277.4 ± 1.7	8	276.6 ± 3.9	7	
340	05 39 26.04	−69 24 47.1	O9.7 II-Ib	270.5 ± 3.7	5	266.6 ± 5.5	4	
341	05 39 28.52	−69 27 10.2	B1 Ib Nwk	260.0 ± 3.6	7	265.0 ± 2.5	5	
343	05 39 31.26	−69 21 54.6	O8 II(f)	275.1 ± 3.0	6	278.4 ± 7.4	4	
344	05 39 34.96	−69 39 19.3	O6.5-7 III	...	...	257.4 ± 4.4	3	
345	05 39 36.58	−69 28 05.3	O6.5 II(f)(n)	...	...	287.0 ± 2.8	3	BI 260
352	05 39 46.20	−69 38 52.7	Mid-O V	...	...	258.6 ± 6.1	3	F09 048
353	05 39 46.32	−69 21 07.8	B0.7 Ib Nwk	255.8 ± 2.1	8	256.9 ± 2.3	6	
355	05 39 54.52	−68 37 12.8	B0.7 II-Ib	269.7 ± 1.5	7	269.1 ± 3.7	4	
356	05 39 55.79	−69 16 25.9	B1 Iab Nstr	249.8 ± 0.6	9	245.7 ± 3.1	6	Sk−69°256
361	05 40 04.60	−69 39 50.6	O5 III(fc)	...	...	243.2 ± 7.4	3	BI 265; F09 082
362	05 40 07.15	−69 26 10.7	O8.5 III((f))	259.5 ± 1.6	5	265.4 ± 4.3	4	
364	05 40 08.21	−69 39 17.1	O4 III(f)	254.2 ± 3.0	3	262.0 ± 2.7	3	F09 088
367	05 40 12.76	−68 59 29.8	O5-6 III(f)	275.4 ± 5.3	3	270.5 ± 2.9	3	BI 254
368	05 40 13.79	−69 25 34.6	O7.5n(f)p	...	...	...	...	
369	05 40 24.73	−69 40 13.2	O5-6 Vz	240.4 ± 4.7	3	257.4 ± 11.1	3	F09 111
371	05 40 32.03	−69 19 45.7	O9.5 II	269.0 ± 3.6	6	269.2 ± 1.7	3	
374	05 40 47.28	−69 20 27.9	Early B + early B	Binary (SB2)				
375	05 40 56.32	−68 30 35.5	B1.5 Ib	288.3 ± 0.7	9	291.0 ± 1.5	5	Sk−68°147
376	05 40 59.78	−69 38 40.3	B1.5 Ia Nwk	249.8 ± 1.2	9	238.9 ± 0.5	5	Sk−69°268; F09 147
377	05 41 06.55	−69 40 22.0	B1.5 Ib	254.6 ± 1.7	9	252.6 ± 1.3	5	Sk−69°269; F09 150
380	05 41 11.16	−69 55 44.2	O7(n)(f)p	...	...	...	...	Sk−69°269a
381	05 41 11.34	−69 44 31.5	O9 III	207.6 ± 5.6	5	206.3 ± 9.1	4	F09 152
383	05 41 14.30	−69 17 33.0	O9.2 Ib	189.0 ± 5.0	4	...	...	
384	05 41 14.89	−68 41 20.4	B3 Ib	283.7 ± 2.2	9	277.4 ± 2.2	5	
385	05 41 17.42	−68 36 28.3	A0 II-Ib	258.9 ± 7.9	4	261.2 ± 5.6	5	
386	05 41 18.83	−69 31 58.7	B0.5 Ib Nwk	254.4 ± 5.4	5	255.5 ± 5.4	3	
387	05 41 20.10	−69 36 22.9	B5 Ia	264.0 ± 1.2	7	252.4 ± 1.3	5	Sk−69°271; F09 158
389	05 41 28.16	−69 38 07.1	B1 Ib	260.4 ± 1.1	9	263.0 ± 1.5	6	F09 165
390	05 41 29.44	−69 46 22.6	O9.7 Ia	321.4 ± 2.5	3	...	...	F09 166
391	05 41 30.78	−69 40 08.1	B0 Ia	267.5 ± 0.8	8	266.2 ± 2.2	5	F09 168
393	05 41 34.55	−69 19 08.6	B0 Iab	264.1 ± 1.6	8	261.8 ± 5.5	4	
394	05 41 36.78	−70 00 52.4	B0.7 Ia	246.6 ± 1.2	8	258.5 ± 2.7	5	Sk−70°111
397	05 41 40.12	−69 39 51.6	B1 Ib Nwk	261.0 ± 1.2	9	264.9 ± 2.1	6	F09 177
398	05 41 40.47	−69 41 47.7	B0.7 III-II	266.3 ± 1.9	8	255.8 ± 3.5	5	

continued on next page

Table 2. *continued*

Star	α (J2000)	δ (J2000)	Spectral type	$v_1 \pm$ s.e. [km s^{-1}]	n	$v_2 \pm$ s.e. [km s^{-1}]	n	Comments
400	05 41 48.89	−68 54 52.5	B1.5 Ib Nstr	280.6 ± 1.8	8	281.1 ± 0.9	6	
401	05 41 51.52	−68 53 13.5	B0.5 Ia	222.5 ± 2.5	9	216.1 ± 3.2	5	
402	05 41 59.77	−69 31 56.7	B1 Ib(n) Nwk	245.7 ± 13.6	4	262.9 ± 7.6	3	
407	05 42 09.05	−69 12 19.7	O9.5 II	252.8 ± 4.0	6	264.1 ± 5.6	4	In NGC 2100
408	05 42 09.05	−69 13 00.4	B3 Ia	251.1 ± 2.1	7	250.2 ± 1.4	6	In NGC 2100
409	05 42 13.46	−69 15 27.1	O7 III((f))	313.1 ± 2.6	6	313.9 ± 3.7	4	
412	05 42 20.86	−69 29 16.1	A7 II	265.6 ± 5.6	3	262.2 ± 7.6	3	
414	05 42 35.99	−69 04 11.5	O8.5 Iabf (+ OB?)	Binary (SB2?)				Sk−69°287
415	05 42 41.93	−69 31 14.4	B1 Ib(n)	263.8 ± 4.3	5	256.3 ± 5.5	4	
416	05 42 55.49	−69 00 14.0	B0.2-0.5 III:(n)	...	...	277.1 ± 7.1	3	
417	05 42 56.01	−69 27 42.8	O9.2 II	271.5 ± 3.5	6	281.1 ± 8.2	4	Sk−69°291
419	05 42 57.94	−69 26 29.1	B1-1.5 I	452.9 ± 2.7	7	430.0 ± 2.7	3	
421	05 43 04.37	−68 58 57.8	B1 III	253.3 ± 2.1	8	253.6 ± 1.5	4	
422	05 43 10.49	−69 45 54.8	O6-7 Iabf	...	...	...	...	
424	05 43 24.79	−68 56 59.7	B0.7 Ib Nwk	192.2 ± 3.8	7	199.9 ± 2.9	6	Sk−68°157
425	05 43 41.34	−69 37 27.4	O8 III	270.8 ± 3.1	5	266.3 ± 2.5	4	
426	05 43 58.96	−69 30 57.9	O6.5 III(f)	213.6 ± 6.5	5	220.7 ± 6.9	3	Sk−69°295
427	05 44 02.75	−69 26 10.1	B0.7 Iab	243.1 ± 3.7	9	243.9 ± 2.8	6	
428	05 44 12.24	−69 40 46.6	O7.5 V((f))	166.4 ± 2.6	5	163.7 ± 4.1	4	
430	05 45 23.48	−69 46 22.0	O6-7 V	...	...	...	...	

Notes. *Cross-references in final column:* Sanduleak (1969, Sk), Brunet et al. (1975, BI), Stock et al. (1976, SOI), Schild & Testor (1992, ST92[1–4]-##), Parker (1993, P93), Testor & Niemela (1998, ST92 5-##), Fariña et al. (2009, F09) and Evans et al. (2011, VFTS). For all but the last two of these references we have employed Brian Skiff's updated astrometry for cross-identifications (see: ftp://ftp.lowell.edu/pub/bas/starcats/). We also include matches to stars in LH 64, LH 81, LH 85, and LH 89 (Lucke & Hodge 1970) from Massey et al. (2000), in which we include their identifications for sources from Westerlund (1961) where relevant.
Sources of adopted classifications: AAΩ 30 Dor 040: Walborn et al. (2004); *254:* Evans et al. (2010); *276:* Walborn et al. (2014); *142, 187, 320, 333, 368, & 380:* Walborn et al. (2010).
Other relevant comments: AAΩ 30 Dor 015: Sk−68°91a is a pair of stars separated by ∼4.″5; the AAOmega spectrum is of the southern star. *AAΩ 30 Dor 283:* Possible contribution from VFTS 172 at 1.″85. *AAΩ 30 Dor 296:* MCPS position is offset ∼0.″66 SE of P93-304/VFTS 389; likely contribution to observed spectrum as well from P93-294/VFTS 386 (∼1.″4 NW). *AAΩ 30 Dor 374:* A preliminary classification of B1 III was given by Muraveva et al. (2014, identified as lm0031122987).

Table 3. MCPS photometry of target stars (Zaritsky et al. 2004).

Star	U	B	V	I_c	$U-B$	$B-V$	$V-I_c$
001	12.293	13.354	13.476	13.864	−1.061	−0.122	−0.388
004	12.635	13.372	13.486	13.729	−0.737	−0.114	−0.243
008	12.896	14.086	13.879	14.013	−1.190	0.207	−0.134
009	12.967	13.713	13.902	14.054	−0.746	−0.189	−0.152
010	12.303	13.274	13.436	13.786	−0.971	−0.162	−0.350
011	12.951	13.624	13.845	13.981	−0.673	−0.221	−0.136
014	11.673	12.754	12.926	13.216	−1.081	−0.172	−0.290
015	11.763	12.734	12.836	13.363	−0.971	−0.102	−0.527
016	12.853	13.484	13.486	13.684	−0.631	−0.002	−0.198
017	12.951	13.703	13.943	13.981	−0.752	−0.240	−0.038
018	13.031	13.780	13.832	13.862	−0.749	−0.052	−0.030
019	12.841	13.717	13.692	13.886	−0.876	0.025	−0.194
020	11.513	12.554	12.726	13.113	−1.041	−0.172	−0.387
021	12.593	13.564	13.706	13.801	−0.971	−0.142	−0.095
024	12.263	13.264	13.406	13.537	−1.001	−0.142	−0.131
025	12.323	13.304	13.426	13.508	−0.981	−0.122	−0.082
026	12.483	13.364	13.436	13.553	−0.881	−0.072	−0.117
027	12.633	13.624	13.756	13.879	−0.991	−0.132	−0.123
028	13.132	13.850	13.926	14.049	−0.718	−0.076	−0.123
030	13.088	14.152	13.853	14.285	−1.064	0.299	−0.432
033	13.332	13.767	13.821	13.951	−0.435	−0.054	−0.130
034	12.243	13.254	13.356	13.431	−1.011	−0.102	−0.075
036	12.889	13.823	13.883	14.101	−0.934	−0.060	−0.218
038	12.663	13.939	13.720	14.064	−1.276	0.219	−0.344
040	12.283	13.444	13.666	13.854	−1.161	−0.222	−0.188
042	13.039	13.682	13.804	13.857	−0.643	−0.122	−0.053
043	12.273	13.204	13.266	13.741	−0.931	−0.062	−0.475
045	13.361	14.071	13.780	13.938	−0.710	0.291	−0.158
047	12.843	13.214	13.216	13.294	−0.371	−0.002	−0.078
049	13.725	13.726	13.473	13.558	−0.001	0.253	−0.085
050	12.658	13.603	13.644	13.873	−0.945	−0.041	−0.229
053	12.491	13.511	13.534	13.829	−1.020	−0.023	−0.295
054	12.636	13.743	13.587	13.651	−1.107	0.156	−0.064
055	12.995	13.633	13.652	13.685	−0.638	−0.019	−0.033
056	12.543	13.474	13.576	13.812	−0.931	−0.102	−0.236
057	12.353	13.444	13.656	13.816	−1.091	−0.212	−0.160
058	12.975	13.737	13.785	14.546	−0.762	−0.048	−0.761
059	13.059	13.869	13.858	14.169	−0.810	0.011	−0.311
060	11.453	12.444	12.546	12.673	−0.991	−0.102	−0.127
061	12.503	13.434	13.546	13.603	−0.931	−0.112	−0.057
062	13.013	13.654	13.778	13.906	−0.641	−0.124	−0.128
063	12.944	13.756	13.801	13.985	−0.812	−0.045	−0.184
064	12.303	13.264	13.376	13.500	−0.961	−0.112	−0.124
065	12.581	13.841	13.911	14.127	−1.260	−0.070	−0.216
068	13.296	13.937	13.947	14.215	−0.641	−0.010	−0.268
069	13.026	13.752	13.928	14.082	−0.726	−0.176	−0.154
071	13.230	13.844	13.841	13.902	−0.614	0.003	−0.061
072	12.622	13.505	13.592	13.705	−0.883	−0.087	−0.113
074	11.903	12.974	13.116	13.259	−1.071	−0.142	−0.143
075	12.836	13.709	13.888	13.908	−0.873	−0.179	−0.020
076	12.987	13.787	13.858	13.953	−0.800	−0.071	−0.095
077	12.797	13.708	13.878	14.143	−0.911	−0.170	−0.265
078	12.293	13.094	13.186	13.210	−0.801	−0.092	−0.024
079	12.824	13.676	13.842	14.043	−0.852	−0.166	−0.201
082	13.710	14.014	13.969	13.985	−0.304	0.045	−0.016
083	11.343	12.304	12.386	12.510	−0.961	−0.082	−0.124
084	12.743	13.674	13.726	14.021	−0.931	−0.052	−0.295
085	12.623	13.634	13.816	13.937	−1.011	−0.182	−0.121
086	12.513	13.434	13.546	13.884	−0.921	−0.112	−0.338
089	13.030	13.858	13.957	13.965	−0.828	−0.099	−0.008
090	14.383	14.274	13.896	14.359	0.109	0.378	−0.463
091	12.583	13.494	13.596	13.687	−0.911	−0.102	−0.091
092	12.043	13.024	13.136	13.290	−0.981	−0.112	−0.154
093	12.675	13.701	13.700	13.883	−1.026	0.001	−0.183
094	12.323	13.314	13.436	13.590	−0.991	−0.122	−0.154
095	13.302	13.717	13.643	13.677	−0.415	0.074	−0.034

continued on next page

Table 3. *continued*

Star	U	B	V	I_c	$U-B$	$B-V$	$V-I_c$
096	12.924	13.752	13.894	14.073	−0.828	−0.142	−0.179
097	12.799	13.709	13.872	14.172	−0.910	−0.163	−0.300
098	12.053	12.814	12.816	12.830	−0.761	−0.002	−0.014
099	12.673	13.544	13.646	13.722	−0.871	−0.102	−0.076
100	12.802	13.590	13.784	13.931	−0.788	−0.194	−0.147
101	13.039	14.082	13.997	14.090	−1.043	0.085	−0.093
103	11.883	12.854	12.956	13.002	−0.971	−0.102	−0.046
104	12.744	13.897	13.647	13.778	−1.153	0.250	−0.131
105	12.130	13.173	13.257	13.417	−1.043	−0.084	−0.160
106	12.473	13.444	13.566	13.650	−0.971	−0.122	−0.084
109	11.853	12.844	12.976	13.134	−0.991	−0.132	−0.158
110	13.023	13.692	13.748	13.992	−0.669	−0.056	−0.244
111	13.024	13.603	13.805	13.981	−0.579	−0.202	−0.176
112	12.443	13.414	13.526	13.552	−0.971	−0.112	−0.026
113	11.703	12.774	12.916	13.088	−1.071	−0.142	−0.172
114	12.968	13.802	13.885	14.177	−0.834	−0.083	−0.292
115	12.413	13.414	13.526	13.689	−1.001	−0.112	−0.163
116	12.313	13.274	13.356	13.539	−0.961	−0.082	−0.183
117	12.884	13.708	13.769	13.835	−0.824	−0.061	−0.066
120	12.473	13.534	13.676	13.758	−1.061	−0.142	−0.082
121	12.243	13.204	13.316	13.459	−0.961	−0.112	−0.143
122	12.123	13.204	13.416	13.435	−1.081	−0.212	−0.019
123	13.175	13.899	13.901	13.948	−0.724	−0.002	−0.047
124	12.980	13.851	13.935	14.164	−0.871	−0.084	−0.229
125	12.956	13.845	13.957	14.242	−0.889	−0.112	−0.285
126	13.237	13.676	13.580	14.436	−0.439	0.096	−0.856
127	12.760	13.795	13.892	14.117	−1.035	−0.097	−0.225
128	13.652	14.095	13.752	13.907	−0.443	0.343	−0.155
129	12.113	13.134	13.246	13.355	−1.021	−0.112	−0.109
130	12.163	13.144	13.246	13.522	−0.981	−0.102	−0.276
132	12.513	13.494	13.586	13.647	−0.981	−0.092	−0.061
133	13.109	13.689	13.623	13.738	−0.580	0.066	−0.115
134	12.774	13.808	13.947	14.051	−1.034	−0.139	−0.104
135	12.843	13.582	13.561	13.868	−0.739	0.021	−0.307
136	11.923	12.924	13.046	13.161	−1.001	−0.122	−0.115
137	12.543	13.254	13.156	13.183	−0.711	0.098	−0.027
138	11.943	12.934	13.026	13.132	−0.991	−0.092	−0.106
139	12.799	13.642	13.619	13.906	−0.843	0.023	−0.287
140	12.313	13.384	13.536	13.638	−1.071	−0.152	−0.102
142	12.003	13.084	13.236	13.411	−1.081	−0.152	−0.175
143	12.563	13.474	13.566	13.606	−0.911	−0.092	−0.040
144	12.283	13.354	13.506	13.647	−1.071	−0.152	−0.141
145	12.404	13.194	13.327	13.640	−0.790	−0.133	−0.313
146	12.860	14.104	13.930	14.089	−1.244	0.174	−0.159
149	12.940	13.791	13.872	13.995	−0.851	−0.081	−0.123
150	13.009	13.864	13.986	14.342	−0.855	−0.122	−0.356
151	12.954	13.603	13.743	13.927	−0.649	−0.140	−0.184
152	11.275	11.910	11.417	12.432	−0.635	0.493	−1.015
155	12.722	13.710	13.853	14.098	−0.988	−0.143	−0.245
157	12.737	13.616	13.793	14.023	−0.879	−0.177	−0.230
159	12.698	13.596	13.702	13.752	−0.898	−0.106	−0.050
160	14.277	14.011	13.695	15.370	0.266	0.316	−1.675
161	12.563	13.384	13.416	13.500	−0.821	−0.032	−0.084
162	12.533	13.464	13.506	13.764	−0.931	−0.042	−0.258
163	12.193	13.234	13.366	13.412	−1.041	−0.132	−0.046
164	11.323	12.163	12.159	12.545	−0.840	0.004	−0.386
168	12.313	13.084	13.136	14.399	−0.771	−0.052	−1.263
169	12.734	13.638	13.807	14.026	−0.904	−0.169	−0.219
170	12.820	13.533	13.752	13.969	−0.713	−0.219	−0.217
172	13.074	13.835	13.917	14.015	−0.761	−0.082	−0.098
173	12.749	12.658	12.518	12.835	0.091	0.140	−0.317
174	12.339	13.188	13.287	13.544	−0.849	−0.099	−0.257
176	13.341	14.071	13.940	14.025	−0.730	0.131	−0.085
177	13.119	13.866	13.922	14.162	−0.747	−0.056	−0.240
178	12.507	13.349	13.297	13.726	−0.842	0.052	−0.429
179	13.308	14.121	13.634	13.968	−0.813	0.487	−0.334
180	11.963	12.924	13.056	13.175	−0.961	−0.132	−0.119

continued on next page

Table 3. *continued*

Star	U	B	V	I_c	$U-B$	$B-V$	$V-I_c$
181	12.335	13.139	13.280	13.514	−0.804	−0.141	−0.234
182	13.204	13.868	13.887	14.062	−0.664	−0.019	−0.175
183	11.823	12.784	12.856	12.893	−0.961	−0.072	−0.037
184	12.951	13.743	13.824	14.065	−0.792	−0.081	−0.241
185	12.713	13.247	13.251	13.536	−0.534	−0.004	−0.285
186	13.263	13.892	13.948	13.989	−0.629	−0.056	−0.041
187	12.113	13.214	13.396	13.481	−1.101	−0.182	−0.085
189	10.981	11.735	11.567	11.833	−0.754	0.168	−0.266
190	11.163	11.904	11.606	12.880	−0.741	0.298	−1.274
192	12.579	13.507	13.520	13.809	−0.928	−0.013	−0.289
194	11.993	13.064	13.086	13.124	−1.071	−0.022	−0.038
195	13.141	13.846	13.827	13.910	−0.705	0.019	−0.083
196	12.948	13.905	13.870	14.117	−0.957	0.035	−0.247
197	14.084	13.274	13.386	13.517	0.810	−0.112	−0.131
199	13.254	13.897	13.990	14.019	−0.643	−0.093	−0.029
200	12.593	13.604	13.726	13.896	−1.011	−0.122	−0.170
201	13.092	13.894	13.990	14.204	−0.802	−0.096	−0.214
206	12.840	13.697	13.775	13.904	−0.857	−0.078	−0.129
207	13.062	13.957	13.937	14.334	−0.895	0.020	−0.397
208	11.923	12.944	13.016	13.456	−1.021	−0.072	−0.440
214	12.573	13.316	13.613	13.772	−0.743	−0.297	−0.159
217	12.273	13.304	13.426	13.473	−1.031	−0.122	−0.047
218	12.750	13.667	13.704	14.110	−0.917	−0.037	−0.406
222	11.573	12.614	12.726	12.928	−1.041	−0.112	−0.202
226	12.836	13.833	13.847	14.080	−0.997	−0.014	−0.233
228	13.016	13.890	13.936	14.262	−0.874	−0.046	−0.326
229	12.073	13.074	13.156	13.264	−1.001	−0.082	−0.108
232	12.330	13.163	13.166	13.433	−0.833	−0.003	−0.267
233	13.146	14.000	13.981	14.301	−0.854	0.019	−0.320
235	12.133	13.124	13.306	13.785	−0.991	−0.182	−0.479
236	12.969	13.819	13.917	14.049	−0.850	−0.098	−0.132
237	12.493	13.494	13.506	13.515	−1.001	−0.012	−0.009
239	14.003	13.874	13.546	13.599	0.129	0.328	−0.053
241	12.811	13.799	13.939	14.169	−0.988	−0.140	−0.230
248	12.023	13.084	13.206	13.209	−1.061	−0.122	−0.003
250	12.843	13.653	13.599	13.991	−0.810	0.054	−0.392
252	12.859	13.693	13.592	13.747	−0.834	0.101	−0.155
254	12.623	13.584	13.546	13.816	−0.961	0.038	−0.270
256	12.766	13.555	13.656	13.704	−0.789	−0.101	−0.048
257	12.353	13.344	13.416	13.553	−0.991	−0.072	−0.137
258	12.972	13.812	13.742	13.993	−0.840	0.070	−0.251
260	13.018	13.741	13.674	13.870	−0.723	0.067	−0.196
261	13.004	13.818	13.913	14.004	−0.814	−0.095	−0.091
264	12.957	13.679	13.797	13.852	−0.722	−0.118	−0.055
266	13.020	13.925	13.917	13.981	−0.905	0.008	−0.064
267	12.223	13.204	13.356	13.423	−0.981	−0.152	−0.067
271	12.493	13.464	13.486	13.651	−0.971	−0.022	−0.165
272	11.713	12.744	12.826	12.929	−1.031	−0.082	−0.103
273	12.663	13.544	13.516	13.539	−0.881	0.028	−0.023
274	12.467	13.207	13.241	13.265	−0.740	−0.034	−0.024
275	12.868	13.880	13.984	14.166	−1.012	−0.104	−0.182
276	12.765	13.650	13.669	13.742	−0.885	−0.019	−0.073
277	11.818	13.655	13.656	13.696	−1.837	−0.001	−0.040
280	12.990	13.908	13.789	13.803	−0.918	0.119	−0.014
281	12.860	13.760	13.655	13.895	−0.900	0.105	−0.240
282	12.660	13.567	13.658	13.838	−0.907	−0.091	−0.180
283	13.096	13.699	13.840	13.900	−0.603	−0.141	−0.060
284	12.917	13.787	13.724	13.780	−0.870	0.063	−0.056
285	12.283	13.234	13.276	13.425	−0.951	−0.042	−0.149
286	11.212	12.069	12.267	12.370	−0.857	−0.198	−0.103
287	11.243	12.122	12.032	12.107	−0.879	0.090	−0.075
288	13.065	13.955	13.980	14.185	−0.890	−0.025	−0.205
290	13.146	13.927	13.684	13.742	−0.781	0.243	−0.058
291	13.227	14.056	13.920	14.168	−0.829	0.136	−0.248
296	12.123	13.084	12.916	13.727	−0.961	0.168	−0.811
308	12.901	14.010	13.905	14.010	−1.109	0.105	−0.105
315	12.393	13.384	13.466	13.556	−0.991	−0.082	−0.090

continued on next page

Table 3. *continued*

Star	U	B	V	I_c	$U-B$	$B-V$	$V-I_c$
318	12.749	13.702	13.700	13.773	−0.953	0.002	−0.073
320	12.824	13.794	13.746	13.945	−0.970	0.048	−0.199
324	12.713	13.637	13.801	14.087	−0.924	−0.164	−0.286
330	12.832	13.955	13.740	14.177	−1.123	0.215	−0.437
333	11.415	12.374	12.273	12.275	−0.959	0.101	−0.002
334	12.810	13.966	13.551	14.168	−1.156	0.415	−0.617
337	13.008	13.824	13.900	14.027	−0.816	−0.076	−0.127
338	12.712	13.736	13.519	13.855	−1.024	0.217	−0.336
339	12.912	13.767	13.821	13.891	−0.855	−0.054	−0.070
340	11.973	13.034	13.036	13.165	−1.061	−0.002	−0.129
341	13.074	14.352	12.599	14.878	−1.278	1.753	−2.279
343	14.855	13.826	13.771	13.985	1.029	0.055	−0.214
344	13.426	13.883	13.670	13.817	−0.457	0.213	−0.147
345	12.635	13.569	13.522	13.664	−0.934	0.047	−0.142
352	13.216	14.168	13.787	14.096	−0.952	0.381	−0.309
353	13.225	14.048	13.924	14.113	−0.823	0.124	−0.189
355	13.000	13.895	13.917	14.161	−0.895	−0.022	−0.244
356	11.713	12.644	12.666	12.772	−0.931	−0.022	−0.106
361	11.526	12.346	12.375	12.493	−0.820	−0.029	−0.118
362	12.883	13.842	13.956	14.088	−0.959	−0.114	−0.132
364	12.867	13.562	13.629	13.637	−0.695	−0.067	−0.008
367	13.029	13.730	13.892	14.087	−0.701	−0.162	−0.195
368	12.113	13.174	13.296	13.356	−1.061	−0.122	−0.060
369	12.013	12.820	12.365	12.638	−0.807	0.455	−0.273
371	12.805	13.626	13.525	13.651	−0.821	0.101	−0.126
374	13.480	13.934	13.761	14.151	−0.454	0.173	−0.390
375	11.923	12.894	12.966	13.088	−0.971	−0.072	−0.122
376	11.803	12.445	12.242	12.308	−0.642	0.203	−0.066
377	12.839	13.546	13.461	13.572	−0.707	0.085	−0.111
380	12.573	13.416	13.444	13.557	−0.843	−0.028	−0.113
381	12.985	13.758	13.871	14.221	−0.773	−0.113	−0.350
383	12.523	13.534	13.646	13.797	−1.011	−0.112	−0.151
384	12.959	13.698	13.628	13.671	−0.739	0.070	−0.043
385	13.672	13.859	13.799	13.809	−0.187	0.060	−0.010
386	12.881	13.777	13.658	13.896	−0.896	0.119	−0.238
387	11.307	11.790	11.790	11.910	−0.483	0.000	−0.120
389	12.137	12.410	12.848	13.071	−0.273	−0.438	−0.223
390	11.515	12.170	12.285	12.303	−0.655	−0.115	−0.018
391	11.673	12.479	12.584	12.945	−0.806	−0.105	−0.361
393	12.143	13.154	13.296	13.406	−1.011	−0.142	−0.110
394	10.812	11.872	11.516	11.965	−1.060	0.356	−0.449
397	12.795	13.507	13.693	13.755	−0.712	−0.186	−0.062
398	13.011	13.739	13.883	14.041	−0.728	−0.144	−0.158
400	12.663	13.514	13.536	13.627	−0.851	−0.022	−0.091
401	11.963	12.954	13.036	13.104	−0.991	−0.082	−0.068
402	13.297	14.086	13.795	14.045	−0.789	0.291	−0.250
407	12.253	13.114	13.156	13.545	−0.861	−0.042	−0.389
408	11.893	12.614	12.566	12.919	−0.721	0.048	−0.353
409	11.923	13.024	13.206	13.372	−1.101	−0.182	−0.166
412	11.453	12.354	12.496	13.112	−0.901	−0.142	−0.616
414	11.333	12.224	12.216	14.113	−0.891	0.008	−1.897
415	13.139	13.961	13.841	13.912	−0.822	0.120	−0.071
416	13.225	13.795	13.954	13.988	−0.570	−0.159	−0.034
417	11.653	12.664	12.696	13.130	−1.011	−0.032	−0.434
419	12.263	13.234	13.256	13.354	−0.971	−0.022	−0.098
421	13.079	13.672	13.703	14.008	−0.593	−0.031	−0.305
422	12.531	13.468	13.321	13.364	−0.937	0.147	−0.043
424	12.173	13.194	13.326	13.408	−1.021	−0.132	−0.082
425	12.857	13.733	13.846	13.983	−0.876	−0.113	−0.137
426	12.572	13.549	13.702	13.826	−0.977	−0.153	−0.124
427	13.090	13.932	13.570	13.587	−0.842	0.362	−0.017
428	12.996	13.819	13.967	14.215	−0.823	−0.148	−0.248
430	12.969	13.947	13.991	14.215	−0.978	−0.044	−0.224

Table 4. Comparison of AAOmega classifications with those available in the literature.

Star	Alias	AAOmega	Published
034	LH64-6	B0.7 Ib(n) Nwk	B1 III [M00]
036	W61 16-6, LH64-7	B1.5 II-Ib(n)	B1: III: [M00]
038	W61 16-7, LH64-33	B1-1.5 V-III	B1 III [M00]
040	W61 16-8, LH64-16	ON2 III(f*)	O3 III:(f*) [M00]; O2 III(f*) [W02]; ON2 III(f*) [W04]
043	W61 16-29	B1 Ib(n) Nwk	B0.2: III: [M00]
047	SOI 624	B9 Ib	A1 Iab [SOI]
049	SOI 625	A5 II	B9 Ib [SOI]
050	W61 16-62, LH64-60	B1 Ib Nwk	B1.5 III [M00]
074	Sk−68° 105	O9.7 Iab	B0 Ia [M95]
078	SOI 399	B3 Iab	A0 Ia [SOI]
084	...	B1.5 Ib Nwk	B1.5 Ib [M14; their lm0020n19615]
106	D226-5	O6.5 V((f))	O6.5 V((f)) [O96b]
112	Sk−68° 117	B1 Iab Nstr	B1 III [M95]
120	Sk−68° 119	O9-9.2 III-II(n)	O9 V [M95]
142	BI 214	O6.5(n)(f)p	O6.5 f [C86]; AAOmega type is from W10
151	LH 81-1018	O9.7 V	B0.5 III [M00]
155	BI 220	O9.7 II(n)	B0.5 III [M95]
159	W61 28-23	O3.5 III(f*)	O3 V((f)) [M00]; O4 III(f+) [W02]; O3.5 V((f+)) [M05]
161	BI 217	B2.5 Ib	B2 III [M95]
170	W61 27-1	B0.2 III(n)	B0.5 III [M00]
179	ST 3-08	B0.2 III(n)	B0 III [ST92]
180	W61 27-7, LH 85-22	B1 Iab Nwk	B1.5: I [M00]
187	...	O6n(f)p	AAOmega type is from W10
195	W61 27-31, LH 89-68, ST92 3-62	B1 Ib Nwk	B1 I [ST92]
200	Sk−68° 127	B0.7 Ib	B0.5 Ia [M95]
214	Sk−69° 216a	O6.5 III(f)	O6 V((f)) [M95]
241	Sk−68° 132	B0 III(n)	B0 V [M95]
254	VFTS 016	O2 III-If*	O2 III-If* [E10]
276	BI 253, VFTS 072	O2 V-III(n)((f*))	O3 V [M95]; O2 V((f*)) [W02]; adopted type is from W14
277	Sk−68° 134	B1 Ib-Iab(n) Nwk?	B1 Ib [M95]
283	ST92 1-72, VFTS 171	O7-8 III((f))	O8 III [ST92]; O8 II-III(f) [W14]
286	Sk−69° 238	O7.5 Ib(f)	O6.5 V((f)) [M95]
287	Sk−69° 237	B1 Ia Nstr	B1 Ia (N str) [F91]
296	P93-304, VFTS 389	O9 III(n)	O8 V [M85]; O8 V [WB97]; O9.5 V [W02b]; O9.5 IV [W14]
308	P93-9017, VFTS 481	O8.5-9 II	O8.5 V [P93]; O8.5 III [W14]
318	ST92 5-85	O8 Ib(f)	O7.5 I(f) [TN98]
320	ST92 5-82	O7n(f)p	O6.5 III [TN98]; AAOmega type is from W10
330	W61 3-9, [M2002] LMC 172231	O9: V-III + O9.5: V-III	O9.5 III [ST92 5-67, TN98]; O9 V + O9.5 V [M12]
333	ST92 5-31	O2-3(n)f*p Nwk	O3 If [TN98]; AAOmega type is from W10 (plus addition of Nwk)
334	ST92 5-25	O5-6 V((f))z	O4 V [TN98]
345	BI 260	O6.5 II(f)(n)	O7 V((f)) [M95]
352	F09 048	Mid-O V	O4-6 Vz [F09]
361	BI 265, F09 082	O5 III(fc)	O6 V [M95]; O5n(f+)p [F09]
364	F09 088	O4 III(f)	O4 III(f) [F09]
367	BI 254	O5-6 III(f)	O8 V [M95]
368	...	O7.5n(f)p	AAOmega type is from W10
369	F09 111	O5-6 Vz	O6: Vz [F09]
374	...	Early B + Early B	B1 III (SB2) [M14; their lm0031122987]
375	Sk−68° 147	B1.5 Ib	B2 II [J01]
376	Sk−69° 268, F09 147	B1.5 Ia Nwk	BC1.5 Iab [F09]
377	Sk−69° 269, F09 150	B1.5 Ib	B1 III: [M95]; B1.5 Iab [F09]
380	Sk−69° 269a	O7(n)(f)p	AAOmega type is from W10
381	F09 152	O9 III	O9 III [F09]
387	Sk−69° 271, F09 158	B5 Ia	B4 III-I [F09]
389	F09 165	B1 Ib	B1.5-2 III-II [F09]
390	F09 166	O9.7 Ia	O9.7 II-Ib [F09]
391	F09 168	B0 Ia	O9.7 Iab [F09]
394	Sk−70° 111	B0.7 Ia	B0.5 Ia [F88,F91]
397	F09 177	B1 Ib Nwk	B1.5 Ib [F09]
417	Sk−69° 291	O9.2 II	B0 III [C86]

Notes. Sources of classifications: SOI (Stock et al. 1976); M85 (Melnick 1985); C86 (Conti et al. 1986); F88 (Fitzpatrick 1988); F91 (Fitzpatrick 1991); M95 (Massey et al. 1995); O96b (Oey 1996b); WB97 (Walborn & Blades 1997); TN98 (Testor & Niemela 1998); M00 (Massey et al. 2000); J01 (Jaxon et al. 2001); W02 (Walborn et al. 2002a); W02b (Walborn et al. 2002b); W04 (Walborn et al. 2004); M05 (Massey et al. 2005); F09 (Fariña et al. 2009); E10 (Evans et al. 2010); W10 (Walborn et al. 2010); M12 (Massey et al. 2012); M14 (Muraveva et al. 2014, which were earlier classifications of the AAOmega spectra by CJE); W14 (Walborn et al. 2014).